Available online at www.sciencedirect.com
SCIENCE DIRECT®
Comput. Methods Appl. Mech. Engrg. 194 (2005) 1797–1822
Computer methods in applied mechanics and engineering
www.elsevier.com/locate/cma

Statical and dynamical behaviour of thin fibre reinforced composite laminates with different shapes

Liz Graciela Nallim [a,*], Sergio Oller Martinez [b], Ricardo Oscar Grossi [a]

[a] CONICET, ICMASA, Facultad de Ingeniería, Universidad Nacional De Salta, Av. Bolivia 5150, 4400 Salta, Argentina
[b] Departamento de Resistencia de Materiales y Estructuras en la Ingeniería, Universidad Politécnica de Cataluña, Campus Norte UPC, Gran Capitán S/N, 08034 Barcelona, Spain

Received 19 April 2004; received in revised form 24 June 2004; accepted 25 June 2004

Abstract

Based on the classical laminated plate theory, a variational approach for the study of the statical and dynamical behaviour of arbitrary quadrilateral anisotropic plates with various boundary conditions is developed. The analytical formulation uses the Ritz method in conjunction with natural coordinates to express the geometry of general plates in a simple form. The deflection of the plate is approximated by a set of beam characteristic orthogonal polynomials generated using the Gram–Schmidt procedure. The algorithm developed is quite general and can be used to study fibre reinforced composite laminates with symmetric lay-ups, which may have general anisotropy and any combinations of clamped, simply supported and free edge support conditions. Various numerical applications are presented and some results are compared with existing values in the literature to demonstrate the accuracy and flexibility of the present method. New results were also determined for plates with different geometrical shapes, combinations of boundary conditions, several stacking sequences and various angles of fibre orientation.

Keywords: Composite plates; Laminates; Ritz method; Free vibration; Mode shapes; Static analysis

1. Introduction

Composite structures, especially laminated composite plates, have been widely used in many engineering advantages of high strength (as well as high stiffness) and light weight. Another advantage of the laminated composite plate is the controllability of the structural properties through changing the fibre orientation

* Corresponding author. Fax: +54 0387 4255351.
E-mail address: lnallim@unsa.edu.ar (L.G. Nallim).

0045-7825/$ - see front matter
doi:10.1016/j.cma.2004.06.009

angles, the number of plies and selecting proper composite materials. With the wide use of composite plate structures in modern industries, dynamic and static analysis of plates of complex geometry becomes an important design procedure. An adequate understanding of the free vibration and the flexural behaviour of these plates components, is crucial to the design and performance evaluation of a mechanical system. However, static and dynamic solutions to these plate problems are strongly dependent on the geometrical shape, boundary conditions and material properties. It is widely recognised that closed form solutions are possible only for a few specific cases [1,2].

Analytical studies about vibration of isotropic and anisotropic plates of different shapes and configurations are well documented. The excellent reviews of Leissa [2,3], Blevins [4] and Bert [5–7], show that most of these results are for isotropic and orthotropic rectangular, circular, elliptical and other regular shaped plates. Nevertheless, analytical studies on general quadrilateral laminated plates with unequal side lengths and different combinations of boundary conditions are rather limited. This may be due to the difficulty in forming a simple and adequate deflection function which can be applied to the entire plate domain and satisfy the boundary conditions. In general, for the analysis of arbitrary shaped plates, several numerical techniques such as finite elements, finite difference and finite strip methods have been deployed by many researchers (see for instance Refs. [8–13]). Although the discretisation methods provide a general framework for the analysis of general plates, they invariably result in problems which possess a large number of degrees of freedom. Therefore, for large scale structural design and analysis, where repeated calculations are often required, one may think of using the Ritz method [14] which, in its conventional form, does not require a mesh generation because only one single super element is used in the whole process. The difficulty associated with the Ritz method is the choice of suitable functions to approximate the deflected shape, which must satisfy the prescribed geometrical boundary conditions of the plates. Bhat [15] proposed a set of beam-characteristic orthogonal polynomials to study the bending deflection of rectangular isotropic plates under static loading. The set of orthogonal polynomials was also used by Bhat [16] to study the free vibration of isotropic rectangular plates. After Bhat contributions', Liew and his co-workers studied the behaviour of different plates using Ritz method with a set of two-dimensional plate functions, which expresses the entire plate domain into two implicitly related variables (see Refs. [17–28]).

The aim of the present paper is to propose a general variational approach using a set of beam characteristic orthogonal polynomials for the static and dynamical analysis of laminated composite plates having different boundary conditions. The analysis is based on the classical Kirchhoff assumptions and the use of natural coordinates in conjunction with the Ritz method to provide one single super-element which expresses the whole plate. In this way, laminates of different geometrical shapes may be represented by the mapping of a square one defined in terms of its natural coordinates. This variational approach allows to investigate the static bending behaviour and the free vibration characteristics of several composite laminated plates with any combination of boundary conditions.

To demonstrate the validity and efficiency of the proposed formulation, several numerical examples are solved and some of them are verified with results from others authors. In addition, a particular case is experimentally verified.

2. Mathematical formulation

2.1. Strain, kinetic and potential energies

Let us consider a flat, thin and composite plate with an arbitrary-shaped quadrilateral planform, as shown in Fig. 1a. The laminate is of uniform thickness h and, in general, is made up of a number of layers each consisting of unidirectional fibre reinforced composite material. The fibre angle of the kth layer counted from the surface $z = -h/2$ is β measured from the x axis to the fibre orientation, with all laminate

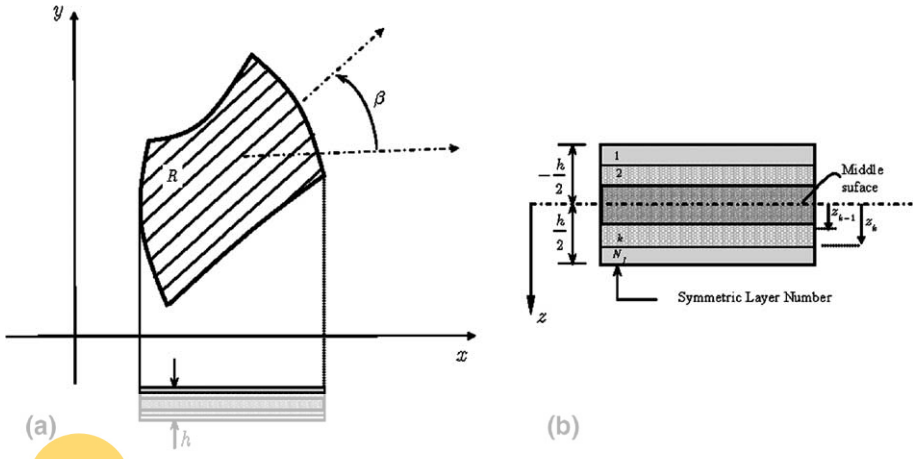

Fig. 1. (a) General description of the composite plate model. (b) Geometry of an N-layered symmetric laminate.

having equal thicknesses. Symmetric lamination of plies are considered, where the fibre angle of each ply is either β or $-\beta$ such that the sequence with respect to the midplane is symmetric (Fig. 1b).

The present study is based on the classical laminated plate theory (CLPT) [29]. In this theory it is assumed that the Kirchhoff hypothesis holds, which requires the displacements in the x, y, z directions, denoted by $\bar{u}, \bar{v}, \bar{w}$ respectively, to be such that

$$\bar{u}(x,y,z,t) = -z\frac{\partial w(x,y,t)}{\partial x}, \quad \bar{v}(x,y,z,t) = -z\frac{\partial w(x,y,t)}{\partial y}, \quad \bar{w}(x,y,z,t) = w(x,y,t), \tag{1}$$

where $w(x,y,t)$ is the mid-plane plate deflection.

The strain energy of the laminated plate can be expressed in rectangular co-ordinates as

$$U = \frac{1}{2}\int\int_R \left[D_{11}\left(\frac{\partial^2 w}{\partial x^2}\right)^2 + 2D_{12}\frac{\partial^2 w}{\partial x^2}\frac{\partial^2 w}{\partial y^2} + D_{22}\left(\frac{\partial^2 w}{\partial y^2}\right)^2 + 4D_{16}\left(\frac{\partial^2 w}{\partial x^2}\frac{\partial^2 w}{\partial x \partial y}\right) + 4D_{26}\left(\frac{\partial^2 w}{\partial y^2}\frac{\partial^2 w}{\partial x \partial y}\right) + 4D_{66}\left(\frac{\partial^2 w}{\partial x \partial y}\right)^2 \right] \mathrm{d}x\,\mathrm{d}y, \tag{2}$$

where the integration is carried out over the entire plate domain R (see Fig. 1a) and D_{ij} are the laminate stiffness coefficients and are obtained by integrating the material properties of each layer of the composite plate [29,30].

The kinetic energy for free transverse vibrations of the plate is given by

$$T = \frac{\rho h}{2}\int\int_R \left(\frac{\partial w}{\partial t}\right)^2 \mathrm{d}x\,\mathrm{d}y, \tag{3}$$

where ρ is the material density, which is considered here to be uniform through the volume of the laminate.

The deflection function is assumed periodic in time; i.e.,

$$w(x,y,t) = W(x,y)\sin\omega t, \tag{4}$$

where ω is the radian natural frequency and $W(x,y)$ is the deflection amplitude of the vibration.

The maximum strain energy $U_{\max}$ and maximum kinetic energy $T_{\max}$ in a vibratory cycle are derived by substituting Eq. (4) into Eqs. (2) and (3), respectively, whence $U_{\max}$ becomes:

$$U_{\max} = \frac{1}{2}\int\int_R \left[D_{11}\left(\frac{\partial^2 W}{\partial x^2}\right)^2 + 2D_{12}\frac{\partial^2 W}{\partial x^2}\frac{\partial^2 W}{\partial y^2} + D_{22}\left(\frac{\partial^2 W}{\partial y^2}\right)^2 + 4D_{16}\left(\frac{\partial^2 W}{\partial x^2}\frac{\partial^2 W}{\partial x \partial y}\right) + 4D_{26}\left(\frac{\partial^2 W}{\partial y^2}\frac{\partial^2 W}{\partial x \partial y}\right) + 4D_{66}\left(\frac{\partial^2 W}{\partial x \partial y}\right)^2 \right] \mathrm{d}x\,\mathrm{d}y, \tag{5}$$

and $T_{\max}$ becomes

$$T_{\max} = \frac{\rho h \omega^2}{2}\int\int_R W^2\,\mathrm{d}x\,\mathrm{d}y. \tag{6}$$

For the statical analysis of the laminate, let us consider the potential energy of a transversal load $q(x,y)$ distributed over the plate surface, which is given by

$$V = -\int\int_R q(x,y) W\,\mathrm{d}x\,\mathrm{d}y. \tag{7}$$

2.2. Transformation of coordinates

An arbitrarily shaped quadrilateral plate in the Cartesian coordinates may be expressed simply by mapping a parent square plate, which will be call master plate, defined in the natural coordinates by the simple boundary equations $\xi = \pm 1$ and $\eta = \pm 1$ (Fig. 2). The mapping of the Cartesian coordinate system is given by [8,9]:

$$x = \sum_{i=1}^{n_p} N_i(\xi,\eta)x_i, \qquad y = \sum_{i=1}^{n_p} N_i(\xi,\eta)y_i \tag{8}$$

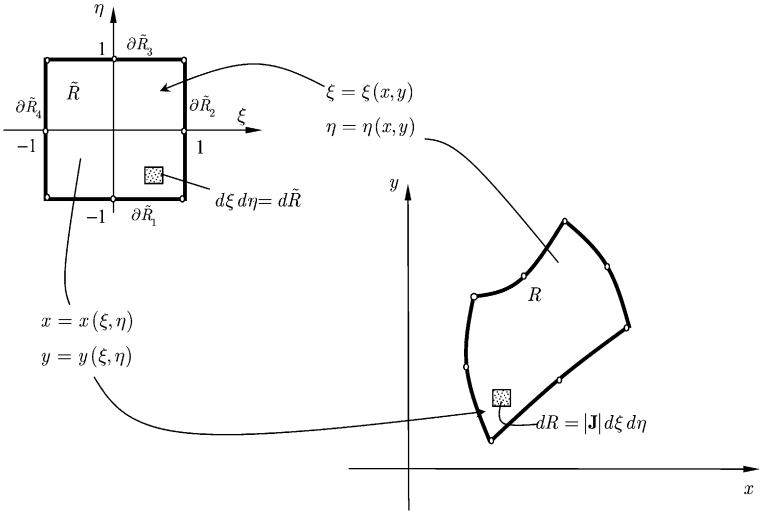

Fig. 2. Mapping of an arbitrary quadrilateral plate into natural coordinates.

where (x_i, y_i), $i = 1, \ldots, n_p$ are the coordinates of n_p points on the boundary of the quadrilateral region R and $N_i(\xi, \eta)$ are the interpolation functions of the serendipity family [8,9]. The transformation (8) maps a point (ξ, η) in the master plate $\tilde{R}$ onto a point (x, y) in the real plate domain R, and vice versa if the Jacobian of the transformation given by:

$$|\mathbf{J}| = \frac{\partial x}{\partial \xi}\frac{\partial y}{\partial \eta} - \frac{\partial x}{\partial \eta}\frac{\partial y}{\partial \xi} \tag{9}$$

is positive.

Applying the chain rule of differentiation it can be shown that the second derivatives of a function $W(x, y)$ are related by

$$\begin{bmatrix} \frac{\partial^2 W}{\partial x^2} \\ \frac{\partial^2 W}{\partial y^2} \\ \frac{\partial^2 W}{\partial x \partial y} \end{bmatrix} = [Op^{(1)}] \begin{bmatrix} \frac{\partial^2 W}{\partial \xi^2} \\ \frac{\partial^2 W}{\partial \eta^2} \\ \frac{\partial^2 W}{\partial \xi \partial \eta} \end{bmatrix} + [Op^{(2)}] \begin{bmatrix} \frac{\partial W}{\partial \xi} \\ \frac{\partial W}{\partial \eta} \end{bmatrix}, \tag{10}$$

where $[Op^{(1)}]$ and $[Op^{(2)}]$ are the derivate transformation matrixes which are defined in Appendix A.

Besides, the elemental area $dx\,dy$ in the real plate domain R is transformed into $|\mathbf{J}|d\xi\,d\eta$. Consequently, the maximum kinetic energy expression given by Eq. (6) and the potential energy given by Eq. (7) reduce, respectively, to:

$$T_{\max} = \frac{h\rho\omega^2}{2}\int_{-1}^{1}\int_{-1}^{1} W^2 |\mathbf{J}|\, d\xi\, d\eta, \tag{11}$$

$$V = -\int_{-1}^{1}\int_{-1}^{1} q(\xi, \eta) W |\mathbf{J}|\, d\xi\, d\eta, \tag{12}$$

where $W = W(\xi, \eta)$.

Finally, substituting the derivatives $\frac{\partial^2 W}{\partial x^2}$, $\frac{\partial^2 W}{\partial y^2}$, $\frac{\partial^2 W}{\partial x \partial y}$ from Eq. (10) into Eq. (5) the maximum strain energy expression becomes

$$\begin{aligned} U_{\max} = \frac{1}{2}\int_{-1}^{1}\int_{-1}^{1}\Bigg[& \left(\frac{\partial^2 W}{\partial \xi^2}\right)^2 S_1 + \left(\frac{\partial^2 W}{\partial \eta^2}\right)^2 S_2 + \frac{\partial^2 W}{\partial \xi^2}\frac{\partial^2 W}{\partial \eta^2} S_3 + \left(\frac{\partial^2 W}{\partial \xi \partial \eta}\right)^2 S_4 \\ & + \frac{\partial^2 W}{\partial \xi^2}\frac{\partial^2 W}{\partial \xi \partial \eta} S_5 + \frac{\partial^2 W}{\partial \eta^2}\frac{\partial^2 W}{\partial \xi \partial \eta} S_6 + \frac{\partial^2 W}{\partial \xi^2}\frac{\partial W}{\partial \xi} S_7 + \frac{\partial^2 W}{\partial \eta^2}\frac{\partial W}{\partial \eta} S_8 + \frac{\partial^2 W}{\partial \xi^2}\frac{\partial W}{\partial \eta} S_9 + \frac{\partial^2 W}{\partial \eta^2}\frac{\partial W}{\partial \xi} S_{10} \\ & + \frac{\partial^2 W}{\partial \xi \partial \eta}\frac{\partial W}{\partial \xi} S_{11} + \frac{\partial^2 W}{\partial \xi \partial \eta}\frac{\partial W}{\partial \eta} S_{12} + \left(\frac{\partial W}{\partial \xi}\right)^2 S_{13} + \left(\frac{\partial W}{\partial \eta}\right)^2 S_{14} + \frac{\partial W}{\partial \xi}\frac{\partial W}{\partial \eta} S_{15} \Bigg] |\mathbf{J}|\, d\xi\, d\eta, \end{aligned} \tag{13}$$

where S_i ($i = 1, \ldots, 15$) are functions that depend on the problem parameters, i.e., geometry and material coefficients of the plate, and are defined in Appendix B.

The total energy functionals for free vibration and transverse bending of the plate are respectively given by:

$$F_d = U_{\max} - T_{\max}, \tag{14a}$$

$$F_s = U + V, \tag{14b}$$

which are to be minimised according to the Ritz principle, as will be discussed in following sections.

2.3. Boundary conditions and the approximating function

Grossi and Nallim [31,32] determined the boundary conditions which correspond to the boundary and the boundary-eingenvalue problems that describe the static and dynamic behaviour of anisotropic plates with non-smooth boundaries. In addition to these geometric and natural boundary conditions which correspond to free, clamped and simply supported edges; they determined that when a plate has a corner formed by the intersection of two free edges, unstable additional corner conditions must be considered. In the application of the Ritz method only the essential boundary conditions are required to be satisfied by the assumed functions [14]. The fact that the natural boundary conditions need not be satisfied by the chosen coordinate functions is a very important characteristic of the Ritz method, specially when dealing with problems for which these satisfaction is very difficult to achieve [33,34]. For instance, this is the case of a rectangular simply supported anisotropic plate where, the Navier analytical solution does not work because of the presence of the bending–twisting coupling: D_{16}, D_{26}.

The use of beam orthogonal polynomials to study anisotropic rectangular plates is very satisfactory, as has been demonstrated by Nallim and Grossi [31,35], since the convergence of the solution is rapid and practically without oscillations. This is also true in the response which requires derivates of the deflections. For this reason, in the present paper the transverse deflection of the plate is expressed in terms of the natural coordinates system by a set of beam characteristic orthogonal polynomials, $\{p_i(\xi)\}$ and $\{q_j(\eta)\}$, as

$$W(\xi,\eta) \approx W_{MN}(\xi,\eta) = \sum_{i=1}^{M}\sum_{j=1}^{N} c_{ij} p_i(\xi) q_j(\eta), \tag{15}$$

where c_{ij} are the unknown coefficients.

The procedure for the construction of the orthogonal polynomials has been developed by Bhat [15,16]. The first members of the set, $p_1(\xi)$ and $q_1(\eta)$ are obtained as the simplest polynomials that satisfy all the geometrical boundary conditions of the plate in their respective ξ and η-directions of the natural coordinate geometry domain to which they are applied. In the present paper, plates having a variety of boundary conditions on the boundary $\partial\tilde{R} = \bigcup_{i=1}^{4}\partial\tilde{R}_i$ are considered. For instance, the geometric boundary conditions for a clamped edge along $\partial\tilde{R}_1$ applied to $q_1(\eta)$ are $q_1(\eta)|_{\eta=-1} = 0$ and $[\partial q_1(\eta)/\partial\eta]|_{\eta=-1} = 0$. For a simply supported edge along $\partial\tilde{R}_2$ there is only one geometric boundary condition given by $p_1(\xi)|_{\xi=1} = 0$. No geometric boundary conditions exist for the free edges.

The starting polynomial of the set in the ξ direction is as follows:

$$p_1(\xi) = \sum_{i=0}^{I} a_i \xi^i, \tag{16}$$

where I is equal to the total number of geometric boundary conditions on the two opposite edges. The arbitrary constants a_i, are determined by substituting Eq. (16) in the corresponding boundary conditions. The starting polynomial of the set in the η direction, $q_1(\eta)$ is constructed in the same way.

The higher members of the set $\{p_i(\xi)\}$ are constructed by employing the Gram–Schmidt orthogonalisation procedure:

$$p_2(\xi) = (\xi - B_2)p_1(\xi), \quad p_k(\xi) = (\xi - B_k)p_{k-1}(\xi) - C_k p_{k-2}(\xi), \tag{17}$$

where

$$B_k = \frac{\int_{-1}^{1} \xi (p_{k-1}(\xi))^2 \,\mathrm{d}\xi}{\int_{-1}^{1} (p_{k-1}(\xi))^2 \,\mathrm{d}\xi}, \quad C_k = \frac{\int_{-1}^{1} \xi p_{k-1}(\xi) p_{k-2}(\xi) \,\mathrm{d}\xi}{\int_{-1}^{1} (p_{k-2}(\xi))^2 \,\mathrm{d}\xi}.$$

The coefficients of the polynomials are chosen in such a way as to make the polynomials orthonormal, $\int_{-1}^{1} p_k^2(\xi) = 1$. The polynomials set along the η direction is also generated using the same procedure.

It is important to point out that working with the master element in natural coordinates allows us to use the same set of orthogonal polynomials for plates of different geometric shapes. This fact makes possible a unified treatment.

3. Application of the Ritz method

The Ritz method is applied to determine analytical approximate solutions for laminated plates of different shapes. For the dynamical analysis the Ritz procedure requires the minimisation of the energy functional (14a) with respect to each of the c_{ij} coefficients

$$\frac{\partial}{\partial c_{ij}}(U_{\max} - T_{\max}) = 0, \quad i,j = 1,\ldots,N,M, \tag{18}$$

where M, N are the numbers of polynomials in each natural co-ordinate.

In the same manner the statical analysis requires the minimisation of the energy functional (14b) with respect to each of the c_{ij} coefficients

$$\frac{\partial}{\partial c_{ij}}(U + V) = 0, \quad i,j = 1,\ldots,N,M. \tag{19}$$

The application of Eq. (18) leads to the following governing eigenvalue equation:

$$\sum_{k=1}^{M}\sum_{h=1}^{N}\left[K_{ijkh} - \omega^2 M_{ijkh}\right]c_{kh} = 0. \tag{20}$$

On the other hand, Eq. (19) leads to the following set of $M \times N$ algebraic equations among c_{kh}

$$\sum_{k=1}^{M}\sum_{h=1}^{N} K_{ijkh}\, c_{kh} - B_{ij} = 0, \tag{21}$$

where

$$K_{ijkh} = \sum_{m=1}^{15} P_{ijkh,m}(\xi,\eta),$$

$$B_{ij} = 2\int_{-1}^{1}\int_{-1}^{1} q(\xi,\eta)p_i(\xi)q_j(\eta)\mid \mathbf{J}\mid \mathrm{d}\xi\,\mathrm{d}\eta,$$

$$M_{ijkh} = 2\rho h\int_{-1}^{1}\int_{-1}^{1} p_i(\xi)p_k(\xi)q_j(\eta)q_h(\eta)\mid \mathbf{J}\mid \mathrm{d}\xi\,\mathrm{d}\eta$$

The details of the deduction of Eqs. (20) and (21) from Eqs. (18) and (19) together with the analytical expressions of the terms P's are given in Appendix C.

Equation (20) yields an eigenvalue determinant, whose zeros give the natural frequencies of the plate. Back substitution yields the coefficient vectors; and finally substitution of these coefficient vectors into Eq. (15) gives the corresponding mode shapes of the plate.

4. Verification and numerical applications

4.1. Generalities

A computer code, based on the variational algorithm developed in this paper, was implemented and used for the analysis of plates having different shapes, material properties and boundary conditions. The presented results correspond to the dynamical and statical analyses of the above mentioned plates. For the dynamical analysis, natural frequencies parameter and modal shapes were computed. While, for the statical analysis, deflections and bending moments were calculated under uniformly distributed loads. Although, in the present study, only plates under uniformly distributed loads are presented, the developed algorithm can handle many others applied loads.

In order to establish the accuracy and applicability of the approach described, numerical results were computed for a number of plate problems for which comparison values were available in the literature. Additionally, a great number of problems were solved and since the number of cases was extremely large, results were presented for only a few cases. Calculations have been performed taking plates with different geometrical shapes, material properties, angles of fibre orientation and stacking sequences.

Let us introduce the terminology to be used throughout the remainder of the paper for describing the boundary conditions of the plates considered. The designation C–S–F–S, for example, identifies a plate with edges (1) clamped, (2) simply supported, (3) free and (4) simply supported (see Fig. 3). The reference flexural rigidity is $D_\beta = E_L h^3/12(1 - \nu_{LT}\nu_{TL})$, the subscripts L and T represent the directions parallel with and perpendicular to the fibre direction.

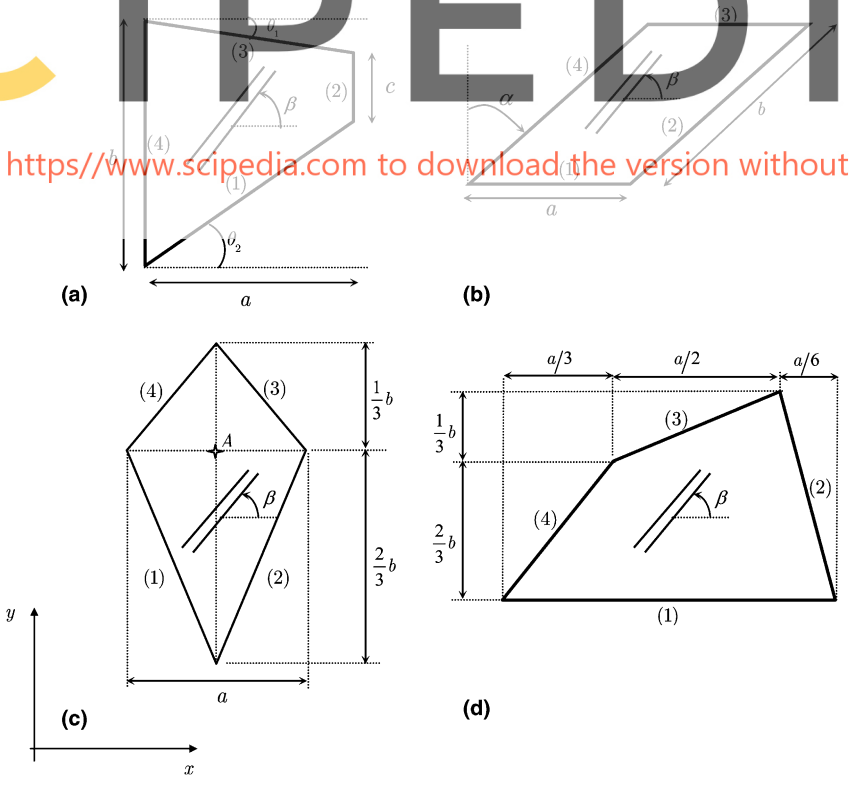

Fig. 3. Laminates of various shapes.

The main purposes of these exercises are twofold. One is to demonstrate the accuracy and efficiency of the proposed method, and the other is to produce some results which may be regarded as benchmark solutions for other academic research workers and design engineers.

4.2. Convergence and comparison of eigenvalues

Results of a convergence study of eigenvalues $\omega a^2\sqrt{\rho h/D_\beta}$ are presented in Table 1. Four-ply E-glass/epoxi laminates (E_L = 60.7 GPa, E_T = 24.8 GPa, G_{LT} = 12 GPa, ν_{LT} = 0.23), with stacking sequence $(\beta,-\beta,-\beta,\beta)$ are considered for β = 30° and 60°. The rate of convergence of eigenvalues is shown for F–S–F–S trapezoidal, skew and rhomboidal laminates. It is well known that the Ritz method gives upper bounds eigenvalues. The convergence of the mentioned eigenvalues is studied by gradually increasing the number of polynomials used in each natural co-ordinate. It can be seen that M, N = 12, is sufficient to reach stable convergence. Moreover, M, N = 10 produces no drastic change in the solutions compared with M, N = 12. Therefore, it was decided to use M, N = 10 to generate the results with sufficient accuracy from an engineering viewpoint.

The accuracy and reliability of the eigenvalues obtained with the presented approach are demonstrated in the following three cases. The comparison presented in Table 2, authenticates the validity of the present method for symmetrically laminated trapezoidal plates with $\theta_1 = \theta_2$ and various chord ratios c/b (see Fig. 3a). The first eight non-dimensional frequencies $\omega ab\sqrt{\rho h/D_\beta}$ for four-ply symmetric laminated plates with stacking sequence $(-\beta,\beta,\beta,-\beta)$ aspect ratio a/b = 2 and subject to two different boundary conditions are tabulated in the mentioned Table. The material properties of each lamina are characterised by E_L/E_T = 40, G_{LT}/E_T = 0.5 and ν_{LT} = 0.25. The results for F–F–F–C plates with β = 30° and 60° are compared to those of Liew and Lim [20], and very good agreement is obtained. All the solutions of Liew and Lim [20] are slightly lower than the present results. This is mainly due to the number of terms used in the approximate shape functions. As stated by Liew and Lim [20], the results reproduced in Table 2 were calculated by using a total of 136 terms for the W shape function. However, 10 characteristic orthogonal polynomials in each natural coordinate were employed in the present study, thus providing a total of 100 terms in the shape function. Other frequencies for S–C–F–S and C–S–S–F four-ply, symmetric laminates are also included in Table 2. The second example considers simply supported and cantilever plates with general shape and parameters (b/a = 1, c/b = 1/2) as shown in Fig. 3a. The first eight non-dimensional frequencies $\omega a^2/h\sqrt{\rho/E_L}$ for four-ply symmetrically laminated E-glass/epoxi plates with stacking sequence $(-\beta,\beta,\beta,-\beta)$, aspect ratio a/b = 2 and subject to two different boundary conditions are tabulated in Table 3. The results for full simply supported and cantilever plates are compared to those of Lim et al. [26], and very good agreement is obtained.

Finally, the third example verifies the accuracy of the eigenvalues for thin skew fibre reinforced laminates with five symmetric angle-ply layers and stacking sequence (45, −45, 45, −45, 45). The geometry of the skew plate is defined by means of a, b and α as shown in Fig. 3b. The material properties of each lamina are E_L/E_T = 40, G_{LT}/E_T = 0.6, ν_{LT} = 0.25 and three skew angles, i.e., α = 0°, 30° and 45°, are used for comparison in this case. The first eight non-dimensional frequencies $\omega(b^2/h\pi^2)\sqrt{\rho/E_T}$ obtained with the present approach, for two kinds of boundary conditions, i.e., fully simply supported (S–S–S–S) and fully clamped (C–C–C–C), are compared with the solutions of Wang [36] in Table 4. Excellent agreement is achieved between both solutions. Additional results for C–F–F–S and S–S–C–F skew laminates, are also included in the mentioned table.

4.3. Comparison of nodal patterns and modal shapes

In this section a comparison between experimental and numerical results obtained with the proposed formulation are shown. The analysed test plate has a general trapezoidal planform, it is made of an isotropic material and it is clamped on edge (4) and the other edges are free. The geometrical and material properties of the plate are specified in Table 5. The experimental results have been obtained using electronic speckle pattern interferometry (ESPI) by the Optical Laser Group (National University of Salta), the details of this

Table 1
Convergence of frequency parameters $\omega a^2\sqrt{\rho h/D_\beta}$ for symmetrically laminated E-glass–epoxi plates with stacking sequence $(\beta, -\beta, -\beta, \beta)$

β	$M \times N$	Mode sequence number							
		1	2	3	4	5	6	7	8
Trapezoidal plate, $a/b = 2$, $c/b = 0.25$, $\theta_1 = \theta_2$									
30°	6 × 6	2.0232	7.4693	9.2771	17.6020	21.2079	31.4849	35.4808	37.6965
	7 × 7	2.0232	7.4692	9.2763	17.4936	21.0931	31.0497	34.8383	37.2965
	8 × 8	2.0232	7.4691	9.2757	17.4897	21.0844	30.6832	34.6169	36.7673
	9 × 9	2.0231	7.4691	9.2755	17.4885	21.0826	30.6643	34.5845	36.7423
	10 × 10	2.0231	7.4691	9.2753	17.4883	21.0820	30.6547	34.5770	36.7288
	11 × 11	2.0231	7.4691	9.2752	17.4884	21.0816	30.6543	34.5760	36.7275
	12 × 12	2.0231	7.4690	9.2751	17.4884	21.0814	30.6542	34.5758	36.7268
60°	5 × 5	1.5957	6.4867	8.4909	15.0218	19.2174	33.1934	40.1868	43.7078
	6 × 6	1.5956	6.4773	8.4802	14.8122	19.1379	27.3909	32.2560	40.1359
	7 × 7	1.5956	6.4771	8.4797	14.6767	19.1012	26.8725	32.1018	39.5945
	8 × 8	1.5956	6.4770	8.4791	14.6715	19.0990	26.1922	31.8788	39.5786
	9 × 9	1.5956	6.4770	8.4789	14.6698	19.0980	26.1592	31.8675	39.4884
	10 × 10	1.5956	6.4770	8.4787	14.6697	19.0976	26.1405	31.8618	39.4838
	11 × 11	1.5956	6.4770	8.4786	14.6696	19.0972	26.1397	31.8607	39.4746
	12 × 12	1.5956	6.4770	8.4784	14.6696	19.0970	26.1395	31.8599	39.4744
Skew plate, $a/b = 1$, $\alpha = 30°$									
30°	6 × 6	9.2318	15.1783	31.3375	37.7032	47.8373	57.7326	76.8751	83.6220
	7 × 7	9.2298	15.1629	31.0927	37.6574	47.5086	56.9774	76.6250	81.9833
	8 × 8	9.2287	15.1599	31.0846	37.6419	47.4558	56.5084	74.8606	81.5083
	9 × 9	9.2282	15.1575	31.0839	37.6396	47.4383	56.4992	74.7724	81.4292
	10 × 10	9.2279	15.1565	31.0827	37.6378	47.4330	56.4966	74.7386	81.4217
	11 × 11	9.2278	15.1556	31.0824	37.6370	47.4294	56.4965	74.7361	81.4203
	12 × 12	9.2277	15.1552	31.0820	37.6364	47.4273	56.4964	74.7343	81.4192
60°	6 × 6	8.4083	12.9744	28.4284	34.6977	45.7578	51.2130	72.9757	81.5947
	7 × 7	8.4004	12.9652	28.3039	34.5442	45.7203	50.5577	72.2518	79.6427
	8 × 8	8.3990	12.9597	28.3017	34.5301	45.6538	50.4242	71.8564	78.0421
	9 × 9	8.3982	12.9560	28.3016	34.5251	45.6333	50.4196	71.8148	77.9019
	10 × 10	8.3978	12.9540	28.3014	34.5219	45.6230	50.4185	71.8077	77.8799
	11 × 11	8.3975	12.9526	28.3014	34.5200	45.6166	50.4183	71.8052	77.8789
	12 × 12	8.3973	12.9516	28.3013	34.5186	45.6122	50.4180	71.8034	77.8787
Rhomboidal plate, $a/b = 1$									
30°	6 × 6	12.6745	26.5317	47.7675	63.2555	75.6158	103.2656	117.0172	136.4726
	7 × 7	12.6744	26.5273	47.7402	62.4949	75.5491	101.8325	115.2071	136.2466
	8 × 8	12.6744	26.5263	47.7384	62.4838	75.5313	101.7452	114.9393	132.4501
	9 × 9	12.6744	26.5255	47.7383	62.4814	75.5295	101.7267	114.9204	132.4088
	10 × 10	12.6744	26.5252	47.7382	62.4802	75.5293	101.7250	114.9138	132.3737
	11 × 11	12.6744	26.5250	47.7382	62.4796	75.5291	101.7246	114.9128	132.3725
	12 × 12	12.6744	26.5249	47.7381	62.4791	75.5290	101.7244	114.9122	132.3717
60°	6 × 6	12.8008	26.3685	48.9445	60.7346	76.6698	107.9375	112.0938	134.5834
	7 × 7	12.8006	26.3434	48.9333	60.1017	76.5243	106.1860	110.7694	134.5029
	8 × 8	12.8006	26.3344	48.9317	60.0845	76.5017	106.1573	110.5055	130.5065
	9 × 9	12.8005	26.3277	48.9315	60.0778	76.4913	106.1316	110.4856	130.4779
	10 × 10	12.8005	26.3242	48.9315	60.0724	76.4862	106.1314	110.4712	130.4293
	11 × 11	12.8005	26.3214	48.9314	60.0697	76.4821	106.1311	110.4642	130.4242
	12 × 12	12.8005	26.3197	48.9314	60.0673	76.4796	106.1311	110.4581	130.4204

Table 2
Frequency parameters $\omega ab\sqrt{\frac{\rho h}{D_\beta}}$ for trapezoidal composite laminates with four symmetric angle-ply layers $(-\beta,\beta,\beta,-\beta)$ and with $a/b = 2$

c/b	β		Mode sequence number							
			1	2	3	4	5	6	7	8
F–F–F–C										
0.25	30°	Present	1.4292	6.5088	11.153	17.447	25.572	34.185	41.231	46.183
		Liew and Lim [20]	1.4285	6.5068	11.150	17.443	25.567	34.178	41.228	46.161
	60°	Present	0.5242	2.5003	6.6330	9.1509	13.133	21.005	22.426	32.954
		Liew and Lim [20]	0.5229	2.4973	6.6286	9.1407	13.127	20.987	22.399	32.763
0.50	30°	Present	1.2114	5.9881	8.2722	16.103	21.037	29.684	33.877	38.347
		Liew and Lim [20]	1.2109	5.9875	8.2713	16.102	21.035	29.683	33.873	38.344
	60°	Present	0.44363	2.3685	6.5152	6.6008	13.226	16.454	22.346	27.560
		Liew and Lim [20]	0.44283	2.3669	6.5092	6.5984	13.222	16.441	22.324	27.539
0.75	30°	Present	1.0890	5.2800	6.7605	14.454	17.553	25.360	26.235	33.702
		Liew and Lim [20]	1.0891	5.2799	6.7618	14.454	17.555	25.359	26.233	33.701
	60°	Present	0.39887	2.2993	4.8515	6.5949	13.083	13.817	22.078	23.712
		Liew and Lim [20]	0.39842	2.2987	4.8475	6.5939	13.077	13.811	22.062	23.699
S–C–F–S										
0.25	30°	Present	8.8250	20.7205	31.2324	39.4444	50.9814	63.5851	7.0219	79.2545
	60°	Present	6.4225	14.0281	23.3516	34.5737	46.2103	49.5273	63.4942	69.0133
0.50	30°	Present	8.1296	18.8568	26.3554	34.8923	44.0993	55.3712	59.5676	68.5765
	60°	Present	5.7021	12.3459	20.6233	30.7605	40.1498	43.5531	54.1623	58.9306
0.75	30°	Present	7.6040	17.1370	23.0643	31.2288	40.1085	49.0695	49.9709	61.5169
	60°	Present	5.1417	11.2012	18.9364	28.5030	33.4761	39.7395	43.6576	52.2321
C–S–S–F										
0.25	30°	Present	13.6706	30.8146	40.3287	51.0371	66.1227	75.9397	86.2925	95.6579
	60°	Present	29.2473	47.6310	64.1050	81.0669	90.0585	108.6065	124.7442	139.090
0.50	30°	Present	12.5154	24.8775	35.4636	40.2675	54.7443	61.6343	73.0903	78.5758
	60°	Present	27.6866	40.7856	51.9092	63.1236	74.7997	84.3329	93.3935	110.552
0.75	30°	Present	11.2647	20.0165	30.9280	34.6424	47.5583	50.1971	62.8488	69.7796
	60°	Present	25.9214	33.5302	40.0809	48.1569	58.5164	71.1055	80.7580	94.9314

experimental technique can be found in Ref. [37]. In Fig. 4 experimentally obtained modal shapes are compared to analytical predictions, obtained with the proposed method for eight of the natural frequencies of free vibration. It can be seen a remarkable agreement between the calculated modal shapes and those obtained by means the ESPI.

4.4. Rhomboidal plates

In this section, results are presented of the developed approach applied to study the statical and dynamical behaviour of rhomboidal laminates as shown in Fig. 3c. The planform geometry of the rhomboidal plate is defined by means of the aspect ratio b/a. Four-ply E-glass/epoxi laminates ($E_L = 60.7$ GPa, $E_T = 24.8$ GPa, $G_{LT} = 12$ GPa, $\nu_{LT} = 0.23$), with stacking sequence $(\beta,-\beta,-\beta,\beta)$ are considered. As shown in Table 6 three different combinations of boundary conditions are taking into account. In each category of

Table 3
Frequency parameters $\frac{\omega a^2}{h}\sqrt{\frac{\rho}{E_L}}$, for general trapezoidal composite laminates with four symmetric angle-ply layers $(-\beta,\beta,\beta,-\beta)$ and with $a/b = 2$

$\frac{c}{b}$	θ_1	β		Mode sequence number							
				1	2	3	4	5	6	7	8
S–S–S–S											
0.25	0°	0°	Present	19.0701	33.8324	50.7168	55.9894	71.9130	82.0421	97.4327	106.214
			Lim et al. [26]	19.070	33.832	50.718	55.988	71.852	82.017	96.895	105.98
		30°	Present	21.1688	35.9472	52.3902	62.9348	72.8788	88.3813	97.8691	114.105
			Lim et al. [26]	21.168	35.947	52.387	62.928	72.741	88.237	97.295	112.86
		60°	Present	23.4112	37.3871	52.9366	69.3333	74.0400	90.5069	99.9535	119.4007
			Lim et al. [26]	23.411	37.386	52.916	69.233	73.926	89.683	99.628	112.27
		90°	Present	23.2906	36.8643	52.0483	68.9188	73.1376	89.0716	99.0967	118.566
			Lim et al. [26]	23.290	36.863	52.020	68.774	73.099	87.969	98.949	109.26
	5°	0°	Present	18.6992	33.4684	50.8896	54.3244	72.2477	80.6193	98.0837	105.4503
			Lim et al. [26]	18.699	33.468	50.890	54.323	72.193	80.607	97.564	105.36
		30°	Present	20.4967	35.4311	52.3098	60.5054	72.8539	87.3175	97.3830	113.2849
			Lim et al. [26]	20.497	35.431	52.308	60.503	72.739	87.263	96.896	112.74
		60°	Present	22.8287	36.9593	52.7782	68.8655	72.1939	90.9500	97.8008	119.9634
			Lim et al. [26]	22.829	36.959	52.763	68.822	72.067	90.295	97.637	113.22
		90°	Present	23.0681	36.6096	51.8279	68.9544	72.1472	88.9842	98.1283	118.5196
			Lim et al. [26]	23.068	36.609	51.802	68.803	72.132	87.975	98.074	109.26
F–F–F–C											
0.5	0°	0°	Present	1.2221	5.6951	6.8472	15.3477	18.5433	28.3769	33.8152	35.6139
			Lim et al. [26]	1.2221	5.6950	6.8471	15.348	18.543	28.376	33.815	35.613
		30°	Present	1.0061	5.2731	6.7338	13.9645	17.8660	26.1989	32.3001	37.4719
			Lim et al. [26]	1.0061	5.2730	6.7339	13.964	17.866	26.197	32.300	37.469
		60°	Present	0.82147	4.44336	6.06730	11.9046	15.7535	22.9109	27.5990	37.1082
			Lim et al. [26]	0.82145	4.4432	6.0671	11.904	15.753	22.909	27.598	37.097
		90°	Present	0.78989	4.2837	5.4574	11.4872	14.2802	22.1285	25.2617	35.8900
			Lim et al. [26]	0.78987	4.2836	5.4573	11.487	14.280	22.128	25.261	35.883
	5°	0°	Present	1.2441	5.8082	6.7956	15.8474	18.2620	29.4464	33.1838	35.3629
			Lim et al. [26]	1.2441	5.8081	6.7955	15.847	18.262	29.446	33.183	35.362
		30°	Present	1.0396	5.4977	6.6585	14.6412	17.7271	27.5625	32.3319	36.3853
			Lim et al. [26]	1.0395	5.4976	6.6585	14.641	17.727	27.561	32.332	36.384
		60°	Present	0.83427	4.5300	6.1437	12.1786	15.9430	23.5677	27.8769	38.4930
			Lim et al. [26]	0.83424	4.5299	6.1435	12.178	15.942	23.566	27.876	38.483
		90°	Present	0.79708	4.3421	5.4137	11.6678	14.1548	22.5941	24.9532	37.0395
			Lim et al. [26]	0.79706	4.3420	5.4136	11.668	14.155	22.593	24.953	37.033

boundary conditions two aspect ratios, i.e., $b/a = 1$ and 2 are considered, and the angle of fibre orientation ranges from $\beta = 0°$ to 90°. In this table, $\beta = 0°$ and 90° mean cross-ply laminates with stacking sequences $(0°,90°,90°,0°)$ or $(90°,0°,0°,90°)$ respectively.

For the statical analysis, deflections and bending moments in an specific point of the rhomboidal plate (point marked by A in Fig. 3c), under uniform distributed load q are calculated. For the dynamical analysis, the first eight natural frequencies of free vibrations are determined.

As can be observed in Table 6, for S–S–S–S laminates with $b/a = 1$ the lowest fundamental frequency occurs for $\beta = 45°$. On the other hand, the maximum values are obtained for the cross-ply configurations. For the same aspect ratio $b/a = 1$, but C–C–C–C boundary condition, the dynamical behaviour of the laminate with regards to the angle of fibre orientation, is quite different. In this case, the fundamental frequency

Table 4
Frequency parameters $\frac{\omega b^2}{h\pi^2}\sqrt{\frac{\rho}{E_T}}$, for skew composite laminates with five symmetric angle-ply layers (45°, −45, 45, −45, 45) and with $a = b$

α		Mode sequence number							
		1	2	3	4	5	6	7	8
S–S–S–S									
0°	Present	2.4339	4.9865	6.1820	8.4869	10.2535	11.6467	12.8259	15.2168
	Wang [36]	2.4339	4.9865	6.1818	8.4870	10.2536	11.6464	12.8260	15.2173
30°	Present	2.6099	5.6869	6.8246	9.4721	11.8822	13.2191	14.2739	17.3240
	Wang [36]	2.6119	5.6902	6.8316	9.4773	11.8900	13.2355	14.2809	17.3382
45°	Present	3.3192	6.9005	9.6936	10.7209	15.5313	16.1444	19.3509	21.2960
	Wang [36]	3.3182	6.9002	9.6908	10.7206	15.5318	16.1447	19.3481	21.3005
C–C–C–C									
0°	Present	3.9009	7.1463	8.4583	11.2109	13.3212	14.7414	16.1260	18.8114
	Wang [36]	3.9009	7.1464	8.4585	11.2112	13.3216	14.7425	16.1271	18.8145
30°	Present	4.5389	8.3765	9.8697	12.8450	15.6794	17.4656	18.3284	21.9142
	Wang [36]	4.5431	8.3819	9.8810	12.8533	15.6906	17.4889	18.3396	21.9364
45°	Present	6.3046	10.8189	14.4932	15.4684	21.0550	22.0641	25.8787	27.6348
	Wang [36]	6.3048	10.8193	14.4949	15.4692	21.0620	22.0759	25.8849	27.6869
C–F–F–S									
0°	Present	0.61806	1.7646	2.8216	4.2823	5.2460	6.8291	7.6222	9.3103
30°	Present	0.71969	1.9514	3.1401	4.5279	6.3471	7.6705	8.4890	10.6722
45°	Present	0.67251	2.0793	4.0722	4.4189	7.5341	8.7412	11.1661	11.7505
S–S–C–F									
0°	Present	1.7740	3.6275	5.1019	6.5743	8.0841	10.0992	10.6657	12.4583
30°	Present	2.1794	4.0524	6.5728	7.3611	9.2862	11.6196	13.4776	14.4630
45°	Present	2.8343	4.8471	8.4746	9.1855	12.3188	12.9092	17.7200	18.4634

Table 5
Mechanical and geometrical properties of the general trapezoidal test plate (Fig. 3a)

Geometric planform	$\theta_1 = 29.985°$, $\theta_2 = 11.183°$ $a = 87$ mm, $b = 90$ mm
Thickness	$h = 0.98 \times 10^{-3}$ m
Poisson's modulus	$v = 0.35$
Young's modulus	$E = 6.82 \times 10^{10}$ N/m^2
Flexural rigidity	$D = 6.1$ N m
Mass density per unit volume	$\rho = 2.86 \times 10^3$ kg/m^3

parameter reaches the highest level for $\beta = 45°$ and the lowest level for $\beta = 75°$. However, when the aspect ratio is $b/a = 2$, the variation of the fundamental frequency, is similar for both simply-supported and clamped rhomboidal laminates. In this case, it is observed that the fundamental frequency has its highest value for $\beta = 0°$ in the S–S–S–S laminate and for $\beta = 15°$ in the C–C–C–C laminate. Then, the fundamental frequencies decrease monotonically and reach minimum values for $\beta = 75°$.

Finally, the results for F–S–F–C plates, for both aspect ratios (i.e. $b/a = 1$ and 2), show similar variation of the dynamical behaviour, when β varies from 0° to 90°. The fundamental frequencies have minimum values for $\beta = 15°$ and increase monotonically for $\beta > 15°$. The maximum values occur at $\beta = 90°$. In conclusion, the boundary constraints and the aspect ratio b/a have significant effects on the behaviour of the fundamental frequencies with respect to the angles of fibre orientation.

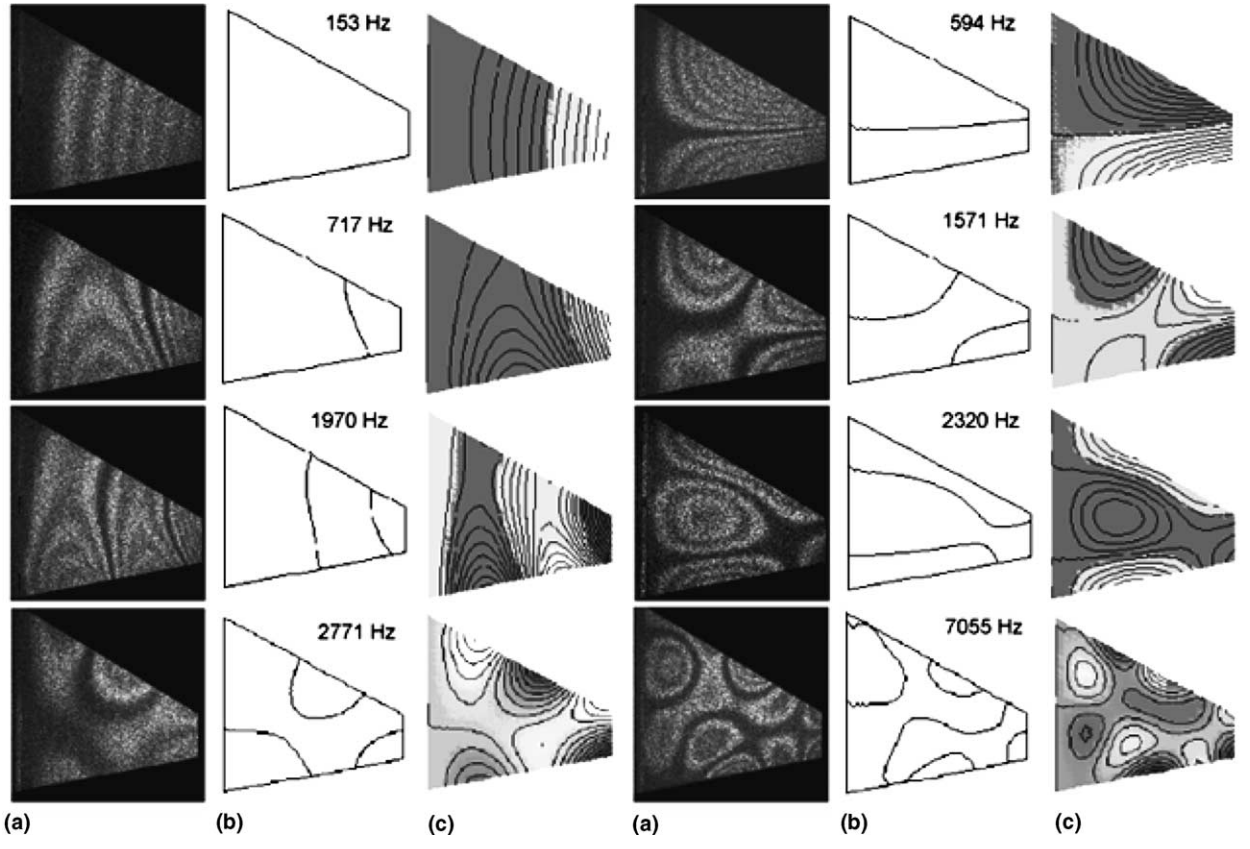

Fig. 4. Natural frequencies and modal shapes of a general trapezoidal cantilever plate. (a) Experimentally determined mode shapes [37]. (b) Nodal patterns obtained with the present method. (c) Modal shapes obtained with the present method.

Table 6
Frequencies of free vibration, static bending deflection and bending moment for four-ply rhomboidal symmetric laminated E-glass–epoxi plates with stacking sequence $(\beta, -\beta, -\beta, \beta)$

b/a	β	Statical analysis		Frequencies of free vibration $\omega a^2\sqrt{\rho h/D_\beta}$							
				Mode sequence number							
		$\frac{WD_\beta}{qa^4}\|_A$	$\frac{M_x}{qa^2}\|_A$	1	2	3	4	5	6	7	8
S–S–S–S											
1	0°	0.00133693	0.02376707	32.8576	75.4172	83.8503	128.528	154.777	156.297	200.106	223.860
	15°	0.00141395	0.02596733	32.0502	72.4077	84.9172	124.163	146.326	164.154	192.890	222.625
	30°	0.00147775	0.02567914	31.3968	71.2486	85.9382	125.305	139.825	170.808	194.618	221.936
	45°	0.00150428	0.02315079	31.0589	70.9395	86.0245	126.585	136.897	173.601	194.546	220.311
	60°	0.00146325	0.01892369	31.3628	71.8190	85.0756	125.927	139.761	171.037	193.214	222.200
	75°	0.00139288	0.01536088	32.0320	73.0827	83.9750	124.846	146.359	164.213	191.461	222.520
	90°	0.00132177	0.01526389	32.8607	75.9610	83.1856	129.063	154.325	156.608	199.122	224.404
2	0°	0.00366604	0.04754341	20.0737	36.6949	56.2655	60.6374	78.8026	92.0729	104.949	121.790
	15°	0.00374594	0.04962897	19.9335	36.3469	55.3904	61.1931	77.2267	92.0566	102.409	121.772
	30°	0.00414294	0.04882469	19.0271	36.1031	55.4023	59.1633	78.3892	89.6005	104.473	117.161
	45°	0.00464907	0.04576604	17.9583	35.7434	53.4624	57.7583	79.7583	86.0722	107.282	110.188
	60°	0.00500802	0.04042163	17.2236	35.5353	50.1564	57.6387	81.1768	82.9676	102.106	110.623
	75°	0.00508757	0.03561888	16.9929	35.4883	47.8736	57.9540	80.6951	82.7449	96.1798	113.446
	90°	0.00469514	0.03581890	17.6523	36.0199	49.6827	58.5220	82.5358	84.1560	98.5616	116.217
C–C–C–C											
1	0°	0.00042582	0.01158452	58.2454	112.062	122.379	174.548	205.928	207.868	257.268	283.315
	15°	0.00042979	0.01215455	58.0819	108.785	125.147	170.721	196.149	218.795	250.273	283.948
	30°	0.00041664	0.01118826	58.8243	108.225	128.858	174.302	189.541	229.261	253.863	286.712
	45°	0.00040787	0.00963926	59.1970	108.212	130.331	177.483	185.940	234.419	254.254	285.375
	60°	0.00040945	0.00807797	58.7931	108.550	128.284	175.028	188.858	230.784	251.345	288.012
	75°	0.00041705	0.00704269	58.0039	109.391	124.142	171.430	195.568	219.788	248.017	283.799
	90°	0.00041507	0.00737193	58.1653	112.883	121.239	175.096	205.294	208.253	255.949	283.539
2	0°	0.00111174	0.02207262	36.8314	58.8535	83.1270	87.6450	109.901	125.523	140.416	159.182
	15°	0.00110060	0.02254566	37.0481	58.5976	82.0608	89.1788	108.280	125.692	137.699	159.292
	30°	0.00115863	0.02137345	36.0536	57.8697	81.2752	87.4305	109.087	122.138	139.372	154.232
	45°	0.00126541	0.01952095	34.4103	56.7976	78.8899	84.7655	109.949	117.102	141.701	146.240
	60°	0.00140589	0.01768004	32.5536	55.6541	74.3086	82.9053	110.424	112.245	135.837	144.122
	75°	0.00152877	0.01651642	31.1404	54.7190	70.1211	81.9192	108.584	110.705	127.178	145.972
	90°	0.00146509	0.01713289	31.8310	55.4846	72.0156	82.6599	110.932	112.336	129.614	149.142

Table 6 (*continued*)

b/*a*	β	Statical analysis		Frequencies of free vibration $\omega a^2\sqrt{\rho h/D_\beta}$							
				Mode sequence number							
		$\frac{WD_\beta}{qa^4}\|_A$	$\frac{M_x}{qa^2}\|_A$	1	2	3	4	5	6	7	8
F–*S*–*F*–*C*											
1	0°	0.00192178	0.02097692	20.0749	35.9246	60.7807	69.0070	98.0648	116.767	129.733	141.435
	15°	0.00222384	0.01947506	18.8546	33.9168	57.7059	67.2526	91.9433	113.083	126.054	138.325
	30°	0.00227301	0.01482298	18.9978	32.3254	58.0007	65.9827	89.2559	114.376	125.899	134.964
	45°	0.00224813	0.01482298	19.3527	31.2364	59.3839	64.1125	88.4524	117.130	123.865	132.590
	60°	0.00221066	0.01122682	19.7787	31.2895	61.3389	62.7327	89.3265	118.306	123.680	131.693
	75°	0.00208758	0.01000555	20.5661	32.2784	62.3017	64.2770	91.8491	115.788	128.965	132.427
	90°	0.00180005	0.01006510	22.0410	34.4608	64.0139	68.5484	97.9682	117.646	133.655	138.400
2	0°	0.00575835	0.05424203	8.51802	19.2463	25.8933	38.1105	43.7022	57.8248	63.5934	75.7244
	15°	0.00671898	0.05168905	8.17785	18.5432	24.8294	37.3132	41.8714	56.5665	60.9715	72.8666
	30°	0.00733401	0.04091217	8.36055	18.2451	24.8001	37.4033	41.7509	57.7187	58.9622	72.4577
	45°	0.00768447	0.03488778	8.54956	17.7511	25.1077	36.9631	42.2672	55.9722	60.5213	71.9866
	60°	0.00802293	0.03481320	8.62899	17.3105	25.6321	36.0528	43.2175	54.2805	62.6014	71.6312
	75°	0.00813069	0.03593550	8.75546	17.3887	26.4330	35.4586	44.6321	54.0893	63.2167	73.3099
	90°	0.00706228	0.03732225	9.19851	18.5509	27.6271	36.8327	46.5567	57.2937	63.6317	77.1701

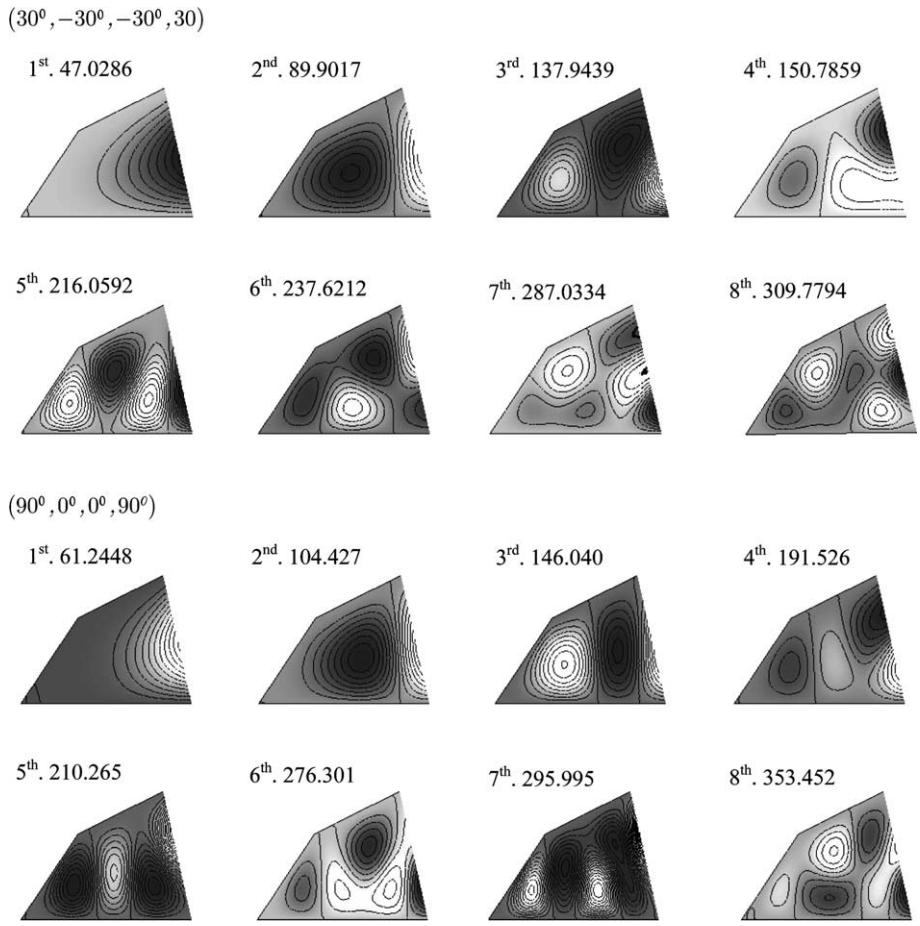

Fig. 5. Transverse vibration frequencies $\omega a^2\sqrt{\rho h/D_\beta}$ and mode shapes of a S–F–C–S general quadrilateral E-glass/epoxi laminate.

4.5. Other quadrilateral plates

The developed Ritz formulation has been further applied to generate results for laminated E-glass/epoxi plates with general quadrilateral planforms (see Fig. 3d). The presented results correspond to a angle-ply laminate with stacking sequence $(30°, -30°, -30°, 30°)$ and to a cross-ply laminate with stacking sequence $(90°, 0°, 0°, 90°)$ and aspect ratio $b/a = 1/2$, for both cases. The plates are simply supported on edges (1) and (4), free on edge (2) and clamped on edge (3). Fig. 5 shows the first eight non-dimensional free vibration frequencies $\omega a^2\sqrt{\rho h/D_\beta}$ and their corresponding modal shapes. It is observed that the frequency parameters are higher for the cross-ply laminate than for the angle-ply laminate. There exist a little difference between the modal shapes for both cases when the first three natural frequencies are considered.

5. Conclusions

A Ritz approach has been developed for the study of the dynamical and statical behaviour of symmetrically laminated composite plates. The proposed method is based on the classical laminated plate theory and

uses natural coordinates to express the geometry of different laminates in a simple form. The deflection of the plate is approximated by a set of beam characteristic orthogonal polynomials generated using the Gram–Schmidt procedure. The algorithm developed is very general and allowed us to take into account a great variety of geometrical shapes, material properties and combinations of classical boundary conditions.

Numerical applications include trapezoidal, skew, rhomboidal and general quadrilateral laminates. For the dynamical analysis frequencies and modal shapes of free vibration have been obtained, and for the statical analysis transverse deflections and bending moments have been determined. For trapezoidal and skew plates, very close agreement was found between the present results and the comparative solutions. Besides, all applications demonstrate that the present technique is accurate and efficient. Consequently it constitutes an efficient tool for the determination of natural frequencies and static deflections in an important number of plate problems, and it is of interest in design works.

Acknowledgement

The authors are indebted to the reviewers of the paper for their constructive comments and suggestions. The present study has been partially sponsored by the Consejo de Investigación, Proyecto CIUNSA 1229.

Appendix A. Coordinate transformation

The definition of the transformation matrixes in Eq. (10), which describe the relation between the derivatives with respect to the Cartesian coordinates (x, y) and the derivatives with respect to the natural coordinates (ξ, η), are obtained applying successively the rule of derivation of composite functions and are given by

$$[Op^{(1)}] = \begin{bmatrix} a'_1 & a'_2 & -a'_3 \\ b'_1 & b'_2 & -b'_3 \\ -c'_1 & -c'_2 & c'_3 \end{bmatrix}, \quad [Op^{(2)}] = \begin{bmatrix} \sum_{i=1}^{3} a'_i\alpha'_i & \sum_{i=1}^{3} a'_i\beta'_i \\ \sum_{i=1}^{3} b'_i\alpha'_i & \sum_{i=1}^{3} b'_i\beta'_i \\ -\sum_{i=1}^{3} c'_i\alpha'_i & -\sum_{i=1}^{3} c'_i\beta'_i \end{bmatrix}$$

where

$$a'_1 = \frac{J_{22}^2}{|\mathbf{J}|^2}, \quad a'_2 = \frac{J_{12}^2}{|\mathbf{J}|^2}, \quad a'_3 = 2\frac{J_{12}J_{22}}{|\mathbf{J}|^2},$$

$$b'_1 = \frac{J_{21}^2}{|\mathbf{J}|^2}, \quad b'_2 = \frac{J_{11}^2}{|\mathbf{J}|^2}, \quad b'_3 = 2\frac{J_{11}J_{21}}{|\mathbf{J}|^2},$$

$$c'_1 = \frac{J_{21}J_{22}}{|\mathbf{J}|^2}, \quad c'_2 = \frac{J_{11}J_{12}}{|\mathbf{J}|^2}, \quad c'_3 = \frac{J_{11}J_{22} + J_{12}J_{21}}{|\mathbf{J}|^2},$$

$$\alpha'_1 = \frac{-J_{11,\xi}J_{22} + J_{12,\xi}J_{21}}{|\mathbf{J}|}, \quad \alpha'_2 = \frac{-J_{21,\eta}J_{22} + J_{22,\eta}J_{21}}{|\mathbf{J}|}, \quad \alpha'_3 = \frac{J_{11,\eta}J_{22} - J_{22,\xi}J_{21}}{|\mathbf{J}|},$$

$$\beta'_1 = \frac{J_{11,\xi}J_{12} - J_{12,\xi}J_{11}}{|\mathbf{J}|}, \quad \beta'_2 = \frac{J_{21,\eta}J_{12} - J_{22,\eta}J_{11}}{|\mathbf{J}|}, \quad \beta'_3 = \frac{J_{11,\eta}J_{12} - J_{22,\xi}J_{11}}{|\mathbf{J}|},$$

$$\mathbf{J}_2 = \begin{bmatrix} \left(\frac{\partial x}{\partial \xi}\right)^2 & \left(\frac{\partial y}{\partial \xi}\right)^2 & 2\frac{\partial x}{\partial \xi}\frac{\partial y}{\partial \xi} \\ \left(\frac{\partial x}{\partial \eta}\right)^2 & \left(\frac{\partial y}{\partial \eta}\right)^2 & 2\frac{\partial x}{\partial \eta}\frac{\partial y}{\partial \eta} \\ \frac{\partial x}{\partial \xi}\frac{\partial x}{\partial \eta} & \frac{\partial y}{\partial \xi}\frac{\partial y}{\partial \eta} & \frac{\partial x}{\partial \xi}\frac{\partial y}{\partial \eta}+\frac{\partial x}{\partial \eta}\frac{\partial y}{\partial \xi} \end{bmatrix} = \begin{bmatrix} J_{11}^2 & J_{12}^2 & 2J_{12}J_{11} \\ J_{21}^2 & J_{22}^2 & 2J_{21}J_{22} \\ J_{11}J_{21} & J_{12}J_{22} & J_{11}J_{22}+J_{21}J_{12} \end{bmatrix},$$

and $|\mathbf{J}|$ denotes the Jacobian determinant.

Appendix B. Definitions of functions S_i in Eq. (13)

After substitution of Eq. (10) into Eq. (5) one obtains the maximum strain energy as a function of the derivatives of the displacement W with respect to the natural coordinates ξ, η. The factors of these derivatives depend on the geometrical and mechanical characteristics of the plates, and are given by

$$S_1(\xi,\eta) = D_{11}a_1'^2 + D_{22}b_1'^2 + 2D_{12}a_1'b_1' + 4D_{66}c_1'^2 - 4D_{16}a_1'c_1' - 4D_{26}b_1'c_1',$$

$$S_2(\xi,\eta) = D_{11}a_2'^2 + D_{22}b_2'^2 + 2D_{12}a_2'b_2' + 4D_{66}c_2'^2 - 4D_{16}a_2'c_2' - 4D_{26}b_2'c_2',$$

$$S_3(\xi,\eta) = 2D_{11}a_1'a_2' + 2D_{22}b_1'b_2' + 2D_{12}(b_1'a_2' + b_2'a_1') + 8D_{66}c_1'c_2' - 4D_{16}(c_2'a_1' + c_1'a_2') - 4D_{26}(b_2'c_1' + b_1'c_2'),$$

$$S_4(\xi,\eta) = D_{11}a_3'^2 + D_{22}b_3'^2 + 2D_{12}a_3'b_3' + 4D_{66}c_3'^2 - 4D_{16}a_3'c_3' - 4D_{26}b_3'c_3',$$

$$S_5(\xi,\eta) = -2D_{11}a_3'a_1' - 2D_{22}b_3'b_1' - 2D_{12}(b_1'a_3' + b_3'a_1') - 8D_{66}c_3'c_1' + 4D_{16}(a_1'c_3' + c_1'a_3') + 4D_{26}(b_3'c_1' + b_1'c_3'),$$

$$S_6(\xi,\eta) = -2D_{11}a_2'a_3' - 2D_{22}b_3'b_2' - 2D_{12}(b_3'a_2' + b_2'a_3') - 8D_{66}c_3'c_2' + 4D_{16}(c_3'a_2' + c_2'a_3') + 4D_{26}(b_3'c_2' + b_2'c_3'),$$

$$\begin{aligned} S_7(\xi,\eta) = {} & 2D_{11}a_1'\sum_{i=1}^{3}a_i'\alpha_i' + 2D_{22}b_1'\sum_{i=1}^{3}b_i'\alpha_i' + 2D_{12}\left(a_1'\sum_{i=1}^{3}b_i'\alpha_i' + b_1'\sum_{i=1}^{3}a_i'\alpha_i'\right) \\ & + 8D_{66}c_1'\sum_{i=1}^{3}c_i'\alpha_i' - 4D_{16}\left(a_1'\sum_{i=1}^{3}c_i'\alpha_i' + c_1'\sum_{i=1}^{3}a_i'\alpha_i'\right) - 4D_{26}\left(b_1'\sum_{i=1}^{3}c_i'\alpha_i' + c_1'\sum_{i=1}^{3}b_i'\alpha_i'\right), \end{aligned}$$

$$\begin{aligned} S_8(\xi,\eta) = {} & 2D_{11}a_2'\sum_{i=1}^{3}a_i'\beta_i' + 2D_{22}b_2'\sum_{i=1}^{3}b_i'\beta_i' + 2D_{12}\left(a_2'\sum_{i=1}^{3}b_i'\beta_i' + b_2'\sum_{i=1}^{3}a_i'\beta_i'\right) \\ & + 8D_{66}c_2'\sum_{i=1}^{3}c_i'\beta_i' - 4D_{16}\left(a_2'\sum_{i=1}^{3}c_i'\beta_i' + c_2'\sum_{i=1}^{3}a_i'\beta_i'\right) - 4D_{26}\left(c_2'\sum_{i=1}^{3}b_i'\beta_i' + b_2'\sum_{i=1}^{3}c_i'\beta_i'\right), \end{aligned}$$

$$\begin{aligned} S_9(\xi,\eta) = {} & 2D_{11}a_1'\sum_{i=1}^{3}a_i'\beta_i' + 2D_{22}b_1'\sum_{i=1}^{3}b_i'\beta_i' + 2D_{12}\left(a_1'\sum_{i=1}^{3}b_i'\beta_i' + b_1'\sum_{i=1}^{3}a_i'\beta_i'\right) \\ & + 8D_{66}c_1'\sum_{i=1}^{3}c_i'\beta_i' - 4D_{16}\left(a_1'\sum_{i=1}^{3}c_i'\beta_i' + c_1'\sum_{i=1}^{3}a_i'\beta_i'\right) - 4D_{26}\left(c_1'\sum_{i=1}^{3}b_i'\beta_i' + b_1'\sum_{i=1}^{3}c_i'\beta_i'\right), \end{aligned}$$

$$S_{10}(\xi,\eta) = 2D_{11}a'_2\sum_{i=1}^{3}a'_i\alpha'_i + 2D_{22}b'_2\sum_{i=1}^{3}b'_i\alpha'_i + 2D_{12}\left(a'_2\sum_{i=1}^{3}b'_i\alpha'_i + b'_2\sum_{i=1}^{3}a'_i\alpha'_i\right)$$
$$+ 8D_{66}c'_2\sum_{i=1}^{3}c'_i\alpha'_i - 4D_{16}\left(a'_2\sum_{i=1}^{3}c'_i\alpha'_i + c'_2\sum_{i=1}^{3}a'_i\alpha'_i\right) - 4D_{26}\left(c'_2\sum_{i=1}^{3}b'_i\alpha'_i + b'_2\sum_{i=1}^{3}c'_i\alpha'_i\right),$$

$$S_{11}(\xi,\eta) = -2D_{11}a'_3\sum_{i=1}^{3}a'_i\alpha'_i - 2D_{22}b'_3\sum_{i=1}^{3}b'_i\alpha'_i - 2D_{12}\left(a'_3\sum_{i=1}^{3}b'_i\alpha'_i + b'_3\sum_{i=1}^{3}a'_i\alpha'_i\right)$$
$$- 8D_{66}c'_3\sum_{i=1}^{3}c'_i\alpha'_i + 4D_{16}\left(a'_3\sum_{i=1}^{3}c'_i\alpha'_i + c'_3\sum_{i=1}^{3}a'_i\alpha'_i\right) + 4D_{26}\left(c'_3\sum_{i=1}^{3}b'_i\alpha'_i + b'_3\sum_{i=1}^{3}c'_i\alpha'_i\right),$$

$$S_{12}(\xi,\eta) = -2D_{11}a'_3\sum_{i=1}^{3}a'_i\beta'_i - 2D_{22}b'_3\sum_{i=1}^{3}b'_i\beta'_i - 2D_{12}\left(a'_3\sum_{i=1}^{3}b'_i\beta'_i + b'_3\sum_{i=1}^{3}a'_i\beta'_i\right)$$
$$- 8D_{66}c'_3\sum_{i=1}^{3}c'_i\beta'_i + 4D_{16}\left(a'_3\sum_{i=1}^{3}c'_i\beta'_i + c'_3\sum_{i=1}^{3}a'_i\beta'_i\right) + 4D_{26}\left(c'_3\sum_{i=1}^{3}b'_i\beta'_i + b'_3\sum_{i=1}^{3}c'_i\beta'_i\right),$$

$$S_{13}(\xi,\eta) = D_{11}\left(\sum_{i=1}^{3}a'_i\alpha'_i\right)^2 + D_{22}\left(\sum_{i=1}^{3}b'_i\alpha'_i\right)^2 + 2D_{12}\sum_{i=1}^{3}b'_i\alpha'_i\sum_{i=1}^{3}a'_i\alpha'_i$$
$$+ 4D_{66}\left(\sum_{i=1}^{3}c'_i\alpha'_i\right)^2 - 4D_{16}\sum_{i=1}^{3}c'_i\alpha'_i\sum_{i=1}^{3}a'_i\alpha'_i - 4D_{26}\sum_{i=1}^{3}b'_i\alpha'_i\sum_{i=1}^{3}c'_i\alpha'_i,$$

$$S_{14}(\xi,\eta) = D_{11}\left(\sum_{i=1}^{3}a'_i\beta'_i\right)^2 + D_{22}\left(\sum_{i=1}^{3}b'_i\beta'_i\right)^2 + 2D_{12}\sum_{i=1}^{3}b'_i\beta'_i\sum_{i=1}^{3}a'_i\beta'_i$$
$$+ 4D_{66}\left(\sum_{i=1}^{3}c'_i\beta'_i\right)^2 - 4D_{16}\sum_{i=1}^{3}c'_i\beta'_i\sum_{i=1}^{3}a'_i\beta'_i - 4D_{26}\sum_{i=1}^{3}b'_i\beta'_i\sum_{i=1}^{3}c'_i\beta'_i,$$

$$S_{15}(\xi,\eta) = 2D_{11}\sum_{i=1}^{3}a'_i\alpha'_i\sum_{i=1}^{3}a'_i\beta'_i + 2D_{22}\sum_{i=1}^{3}b'_i\alpha'_i\sum_{i=1}^{3}b'_i\beta'_i + 2D_{12}\left(\sum_{i=1}^{3}b'_i\beta'_i\sum_{i=1}^{3}a'_i\alpha'_i + \sum_{i=1}^{3}b'_i\alpha'_i\sum_{i=1}^{3}a'_i\beta'_i\right)$$
$$+ 8D_{66}\sum_{i=1}^{3}c'_i\alpha'_i\sum_{i=1}^{3}c'_i\beta'_i - 4D_{16}\left(\sum_{i=1}^{3}c'_i\beta'_i\sum_{i=1}^{3}a'_i\alpha'_i + \sum_{i=1}^{3}c'_i\alpha'_i\sum_{i=1}^{3}a'_i\beta'_i\right)$$
$$- 4D_{26}\left(\sum_{i=1}^{3}b'_i\beta'_i\sum_{i=1}^{3}c'_i\alpha'_i + \sum_{i=1}^{3}b'_i\alpha'_i\sum_{i=1}^{3}c'_i\beta'_i\right),$$

where D_{ij} $(i,j = 1,2,6)$ are the conventional laminate stiffness coefficients and $a'_i, b'_i, c'_i, \alpha'_i, \beta'_i, (i = 1,\ldots,3)$ are defined in Appendix A.

Appendix C. Minimisation of energy functionals

In this Appendix the minimisation of the energy functionals as given in equations (18) and (19) are detailed.

For minimisation purpose, first we replace the approximating function (15) into the expression of $U_{\max}$ given by Eq. (13), as follows

$$
\begin{aligned}
U_{\max} = \frac{1}{2}\int_{-1}^{1}\int_{-1}^{1}\Bigg\{ & S_1\left(\sum_{i,j=1}^{M,N} c_{ij}\frac{\mathrm{d}^2 p_i(\xi)}{\mathrm{d}\xi^2}q_j(\eta)\right)^2 + S_2\left(\sum_{i,j=1}^{M,N} c_{ij}p_i(\xi)\frac{\mathrm{d}^2 q_j(\eta)}{\mathrm{d}\eta^2}\right)^2 \\
& + S_3\left(\sum_{i,j=1}^{M,N} c_{ij}\frac{\mathrm{d}^2 p_i(\xi)}{\mathrm{d}\xi^2}q_j(\eta)\right)\left(\sum_{i,j=1}^{M,N} c_{ij}p_i(\xi)\frac{\mathrm{d}^2 q_j(\eta)}{\mathrm{d}\eta^2}\right) \\
& + S_4\left(\sum_{i,j=1}^{M,N} c_{ij}\frac{\mathrm{d}p_i(\xi)}{\mathrm{d}\xi}\frac{\mathrm{d}q_j(\eta)}{\mathrm{d}\eta}\right)^2 \\
& + S_5\left(\sum_{i,j=1}^{M,N} c_{ij}\frac{\mathrm{d}^2 p_i(\xi)}{\mathrm{d}\xi^2}q_j(\eta)\right)\left(\sum_{i,j=1}^{M,N} c_{ij}\frac{\mathrm{d}p_i(\xi)}{\mathrm{d}\xi}\frac{\mathrm{d}q_j(\eta)}{\mathrm{d}\eta}\right) \\
& + S_6\left(\sum_{i,j=1}^{M,N} c_{ij}p_i(\xi)\frac{\mathrm{d}^2 q_j(\eta)}{\mathrm{d}\eta^2}\right)\left(\sum_{i,j=1}^{M,N} c_{ij}\frac{\mathrm{d}p_i(\xi)}{\mathrm{d}\xi}\frac{\mathrm{d}q_j(\eta)}{\mathrm{d}\eta}\right) \\
& + S_7\left(\sum_{i,j=1}^{M,N} c_{ij}\frac{\mathrm{d}^2 p_i(\xi)}{\mathrm{d}\xi^2}q_j(\eta)\right)\left(\sum_{i,j=1}^{M,N} c_{ij}\frac{\mathrm{d}p_i(\xi)}{\mathrm{d}\xi}q_j(\eta)\right) \\
& + S_8\left(\sum_{i,j=1}^{M,N} c_{ij}p_i(\xi)\frac{\mathrm{d}^2 q_j(\eta)}{\mathrm{d}\eta^2}\right)\left(\sum_{i,j=1}^{M,N} c_{ij}p_i(\xi)\frac{\mathrm{d}q_j(\eta)}{\mathrm{d}\eta}\right) \\
& + S_9\left(\sum_{i,j=1}^{M,N} c_{ij}\frac{\mathrm{d}^2 p_i(\xi)}{\mathrm{d}\xi^2}q_j(\eta)\right)\left(\sum_{i,j=1}^{M,N} c_{ij}p_i(\xi)\frac{\mathrm{d}q_j(\eta)}{\mathrm{d}\eta}\right) \\
& + S_{10}\left(\sum_{i,j=1}^{M,N} c_{ij}p_i(\xi)\frac{\mathrm{d}^2 q_j(\eta)}{\mathrm{d}\eta^2}\right)\left(\sum_{i,j=1}^{M,N} c_{ij}\frac{\mathrm{d}p_i(\xi)}{\mathrm{d}\xi}q_j(\eta)\right) \\
& + S_{11}\left(\sum_{i,j=1}^{M,N} c_{ij}\frac{\mathrm{d}p_i(\xi)}{\mathrm{d}\xi}\frac{\mathrm{d}q_j(\eta)}{\mathrm{d}\eta}\right)\left(\sum_{i,j=1}^{M,N} c_{ij}\frac{\mathrm{d}p_i(\xi)}{\mathrm{d}\xi}q_j(\eta)\right) \\
& + S_{12}\left(\sum_{i,j=1}^{M,N} c_{ij}\frac{\mathrm{d}p_i(\xi)}{\mathrm{d}\xi}\frac{\mathrm{d}q_j(\eta)}{\mathrm{d}\eta}\right)\left(\sum_{i,j=1}^{M,N} c_{ij}p_i(\xi)\frac{\mathrm{d}q_i(\eta)}{\mathrm{d}\eta}\right) \\
& + S_{13}\left(\sum_{i,j=1}^{M,N} c_{ij}\frac{\mathrm{d}p_i(\xi)}{\mathrm{d}\xi}q_j(\eta)\right)^2 + S_{14}\left(\sum_{k,h=1}^{M,N} c_{kh}p_i(\xi)\frac{\mathrm{d}q_j(\eta)}{\mathrm{d}\eta}\right)^2 \\
& + S_{15}\left(\sum_{i,j=1}^{M,N} c_{ij}\frac{\mathrm{d}p_i(\xi)}{\mathrm{d}\xi}q_j(\eta)\right)\left(\sum_{i,j=1}^{M,N} c_{ij}p_i(\xi)\frac{\mathrm{d}q_i(\eta)}{\mathrm{d}\eta}\right)\Bigg\}\,|\mathbf{J}|\;\mathrm{d}\xi\,\mathrm{d}\eta,
\end{aligned}
\tag{C.1}
$$

developing de squares and multiplications in (C.1) one obtains

$$
\begin{aligned}
U_{\max} = \frac{1}{2}\int_{-1}^{1}\int_{-1}^{1}\Bigg\{ & S_1\left(\sum_{k,h=1}^{M,N}\sum_{r,s=1}^{M,N} c_{kh}c_{rs}\frac{\mathrm{d}^2 p_k(\xi)}{\mathrm{d}\xi^2}q_h(\eta)\frac{\mathrm{d}^2 p_r(\xi)}{\mathrm{d}\xi^2}q_s(\eta)\right)\\
& + S_2\left(\sum_{k,h=1}^{M,N}\sum_{r,s=1}^{M,N} c_{kh}c_{rs}p_k(\xi)\frac{\mathrm{d}^2 q_h(\eta)}{\mathrm{d}\eta^2}p_r(\xi)\frac{\mathrm{d}^2 q_s(\eta)}{\mathrm{d}\eta^2}\right)\\
& + S_3\left(\sum_{k,h=1}^{M,N}\sum_{r,s=1}^{M,N} c_{kh}c_{rs}\frac{\mathrm{d}^2 p_k(\xi)}{\mathrm{d}\xi^2}q_h(\eta)p_r(\xi)\frac{\mathrm{d}^2 q_s(\eta)}{\mathrm{d}\eta^2}\right)\\
& + S_4\left(\sum_{k,h=1}^{M,N}\sum_{r,s=1}^{M,N} c_{kh}c_{rs}\frac{\mathrm{d}p_k(\xi)}{\mathrm{d}\xi}\frac{\mathrm{d}q_h(\eta)}{\mathrm{d}\eta}\frac{\mathrm{d}p_r(\xi)}{\mathrm{d}\xi}\frac{\mathrm{d}q_r(\eta)}{\mathrm{d}\eta}\right)\\
& + S_5\left(\sum_{k,h=1}^{M,N}\sum_{r,s=1}^{M,N} c_{kh}c_{rs}\frac{\mathrm{d}^2 p_k(\xi)}{\mathrm{d}\xi}q_h(\eta)\frac{\mathrm{d}p_r(\xi)}{\mathrm{d}\xi}\frac{\mathrm{d}q_s(\eta)}{\mathrm{d}\eta}\right)\\
& + S_6\left(\sum_{k,h=1}^{M,N}\sum_{r,s=1}^{M,N} c_{kh}c_{rs}p_k(\xi)\frac{\mathrm{d}^2 q_h(\eta)}{\mathrm{d}\eta^2}\frac{\mathrm{d}p_r(\xi)}{\mathrm{d}\xi}\frac{\mathrm{d}q_s(\eta)}{\mathrm{d}\eta}\right)\\
& + S_7\left(\sum_{k,h=1}^{M,N}\sum_{r,s=1}^{M,N} c_{kh}c_{rs}\frac{\mathrm{d}^2 p_k(\xi)}{\mathrm{d}\xi^2}q_h(\eta)\frac{\mathrm{d}p_r(\xi)}{\mathrm{d}\xi}q_s(\eta)\right)\\
& + S_8\left(\sum_{k,h=1}^{M,N}\sum_{r,s=1}^{M,N} c_{kh}c_{rs}p_k(\xi)\frac{\mathrm{d}^2 q_h(\eta)}{\mathrm{d}\eta^2}p_r(\xi)\frac{\mathrm{d}q_s(\eta)}{\mathrm{d}\eta}\right)\\
& + S_9\left(\sum_{k,h=1}^{M,N}\sum_{r,s=1}^{M,N} c_{kh}c_{rs}\frac{\mathrm{d}^2 p_k(\xi)}{\mathrm{d}\xi^2}q_h(\eta)p_r(\xi)\frac{\mathrm{d}q_s(\eta)}{\mathrm{d}\eta}\right)\\
& + S_{10}\left(\sum_{k,h=1}^{M,N}\sum_{r,s=1}^{M,N} c_{kh}c_{rs}p_k(\xi)\frac{\mathrm{d}^2 q_h(\eta)}{\mathrm{d}\eta^2}\frac{\mathrm{d}p_r(\xi)}{\mathrm{d}\xi}q_s(\eta)\right)\\
& + S_{11}\left(\sum_{k,h=1}^{M,N}\sum_{r,s=1}^{M,N} c_{kh}c_{rs}\frac{\mathrm{d}p_k(\xi)}{\mathrm{d}\xi}\frac{\mathrm{d}q_h(\eta)}{\mathrm{d}\eta}\frac{\mathrm{d}p_r(\xi)}{\mathrm{d}\xi}q_s(\eta)\right)\\
& + S_{12}\left(\sum_{k,h=1}^{M,N}\sum_{r,s=1}^{M,N} c_{kh}c_{rs}\frac{\mathrm{d}p_k(\xi)}{\mathrm{d}\xi}\frac{\mathrm{d}q_h(\eta)}{\mathrm{d}\eta}p_r(\xi)\frac{\mathrm{d}q_s(\eta)}{\mathrm{d}\eta}\right)\\
& + S_{13}\left(\sum_{k,h=1}^{M,N}\sum_{r,s=1}^{M,N} c_{kh}c_{rs}\frac{\mathrm{d}p_k(\xi)}{\mathrm{d}\xi}q_h(\eta)\frac{\mathrm{d}p_r(\xi)}{\mathrm{d}\xi}q_s(\eta)\right)\\
& + S_{14}\left(\sum_{k,h=1}^{M,N}\sum_{r,s=1}^{M,N} c_{kh}c_{rs}p_k(\xi)\frac{\mathrm{d}q_h(\eta)}{\mathrm{d}\eta}p_r(\xi)\frac{\mathrm{d}q_s(\eta)}{\mathrm{d}\eta}\right)\\
& + S_{15}\left(\sum_{k,h=1}^{M,N}\sum_{r,s=1}^{M,N} c_{kh}c_{rs}\frac{\mathrm{d}p_k(\xi)}{\mathrm{d}\xi}q_h(\eta)p_r(\xi)\frac{\mathrm{d}q_s(\eta)}{\mathrm{d}\eta}\right)\Bigg\}\,|\mathbf{J}|\,\mathrm{d}\xi\,\mathrm{d}\eta. \qquad \text{(C.2)}
\end{aligned}
$$

Then, the derivation of Eq. (C.2) with respect to each coefficient c_{ij}, $i,j = 1, \ldots, N, M$ leads to

$$\begin{aligned}
\frac{\partial U_{\max}}{\partial c_{ij}} = \frac{1}{2}\int_{-1}^{1}\int_{-1}^{1}\Bigg\{ & 2S_1 \sum_{k,h=1}^{M,N} c_{kh}\frac{\mathrm{d}^2 p_i(\xi)}{\mathrm{d}\xi^2}\frac{\mathrm{d}^2 p_k(\xi)}{\mathrm{d}\xi^2} q_j(\eta) q_h(\eta) + 2S_2 \sum_{k,h=1}^{M,N} c_{kh} p_i(\xi) p_k(\xi) \frac{\mathrm{d}^2 q_j(\eta)}{\mathrm{d}\eta^2}\frac{\mathrm{d}^2 q_h(\eta)}{\mathrm{d}\eta^2} \\
& + S_3 \sum_{k,h=1}^{M,N} c_{kh}\left(\frac{\mathrm{d}^2 p_i(\xi)}{\mathrm{d}\xi^2} p_k(\xi)\frac{\mathrm{d}^2 q_j(\eta)}{\mathrm{d}\eta^2} q_h(\eta) + \frac{\mathrm{d}^2 p_k(\xi)}{\mathrm{d}\xi^2} p_i(\xi)\frac{\mathrm{d}^2 q_h(\eta)}{\mathrm{d}\eta^2} q_j(\eta)\right) \\
& + 2S_4 \sum_{k,h=1}^{M,N} c_{kh}\frac{\mathrm{d}p_i(\xi)}{\mathrm{d}\xi}\frac{\mathrm{d}p_k(\xi)}{\mathrm{d}\xi}\frac{\mathrm{d}q_j(\eta)}{\mathrm{d}\eta}\frac{\mathrm{d}q_h(\eta)}{\mathrm{d}\eta} \\
& + S_5 \sum_{k,h=1}^{M,N} c_{kh}\left(\frac{\mathrm{d}^2 p_i(\xi)}{\mathrm{d}\xi^2}\frac{\mathrm{d}p_k(\xi)}{\mathrm{d}\xi} q_j(\eta)\frac{\mathrm{d}q_h(\eta)}{\mathrm{d}\eta} + \frac{\mathrm{d}^2 p_k(\xi)}{\mathrm{d}\xi^2}\frac{\mathrm{d}p_i(\xi)}{\mathrm{d}\xi} q_h(\eta)\frac{\mathrm{d}q_j(\eta)}{\mathrm{d}\eta}\right) \\
& + S_6 \sum_{k,h=1}^{M,N} c_{kh}\left(p_i(\xi)\frac{\mathrm{d}p_k(\xi)}{\mathrm{d}\xi}\frac{\mathrm{d}^2 q_j(\eta)}{\mathrm{d}\eta^2}\frac{\mathrm{d}q_h(\eta)}{\mathrm{d}\eta} + p_k(\xi)\frac{\mathrm{d}p_i(\xi)}{\mathrm{d}\xi}\frac{\mathrm{d}^2 q_h(\eta)}{\mathrm{d}\eta^2}\frac{\mathrm{d}q_j(\eta)}{\mathrm{d}\eta}\right) \\
& + S_7 \sum_{k,h=1}^{M,N} c_{kh} q_j(\eta) q_h(\eta)\left(\frac{\mathrm{d}^2 p_i(\xi)}{\mathrm{d}\xi}\frac{\mathrm{d}p_k(\xi)}{\mathrm{d}\xi} + \frac{\mathrm{d}^2 p_k(\xi)}{\mathrm{d}\xi}\frac{\mathrm{d}p_i(\xi)}{\mathrm{d}\xi}\right) \\
& + S_8 \sum_{k,h=1}^{M,N} c_{kh} p_i(\xi) p_k(\xi)\left(\frac{\mathrm{d}^2 q_j(\eta)}{\mathrm{d}\eta^2}\frac{\mathrm{d}q_h(\eta)}{\mathrm{d}\eta} + \frac{\mathrm{d}^2 q_h(\eta)}{\mathrm{d}\eta^2}\frac{\mathrm{d}q_j(\eta)}{\mathrm{d}\eta}\right) \\
& + S_9 \sum_{k,h=1}^{M,N} c_{kh}\left(\frac{\mathrm{d}^2 p_i(\xi)}{\mathrm{d}\xi^2} p_k(\xi) q_j(\eta)\frac{\mathrm{d}q_h(\eta)}{\mathrm{d}\eta} + \frac{\mathrm{d}^2 p_k(\xi)}{\mathrm{d}\xi^2} p_i(\xi) q_h(\eta)\frac{\mathrm{d}q_j(\eta)}{\mathrm{d}\eta}\right) \\
& + S_{10} \sum_{k,h=1}^{M,N} c_{kh}\left(p_i(\xi)\frac{\mathrm{d}p_k(\xi)}{\mathrm{d}\xi}\frac{\mathrm{d}^2 q_j(\eta)}{\mathrm{d}\eta^2} q_h(\eta) + p_k(\xi)\frac{\mathrm{d}p_i(\xi)}{\mathrm{d}\xi}\frac{\mathrm{d}^2 q_h(\eta)}{\mathrm{d}\eta^2} q_j(\eta)\right) \\
& + S_{11} \sum_{k,h=1}^{M,N} c_{kh}\frac{\mathrm{d}p_i(\xi)}{\mathrm{d}\xi}\frac{\mathrm{d}p_k(\xi)}{\mathrm{d}\xi}\left(\frac{\mathrm{d}q_j(\eta)}{\mathrm{d}\eta} q_h(\eta) + \frac{\mathrm{d}q_h(\eta)}{\mathrm{d}\eta} q_j(\eta)\right) \\
& + S_{12} \sum_{k,h=1}^{M,N} c_{kh}\frac{\mathrm{d}q_j(\eta)}{\mathrm{d}\eta}\frac{\mathrm{d}q_h(\eta)}{\mathrm{d}\eta}\left(\frac{\mathrm{d}p_i(\xi)}{\mathrm{d}\xi} p_k(\xi) + \frac{\mathrm{d}p_k(\xi)}{\mathrm{d}\xi} p_i(\xi)\right) \\
& + S_{13} 2 \sum_{k,h=1}^{M,N} c_{kh}\frac{\mathrm{d}p_i(\xi)}{\mathrm{d}\xi}\frac{\mathrm{d}p_k(\xi)}{\mathrm{d}\xi} q_j(\eta) q_h(\eta) + S_{14} 2 \sum_{k,h=1}^{M,N} c_{kh} p_i(\xi) p_k(\xi)\frac{\mathrm{d}q_j(\eta)}{\mathrm{d}\eta}\frac{\mathrm{d}q_h(\eta)}{\mathrm{d}\eta} \\
& + S_{15} \sum_{k,h=1}^{M,N} c_{kh}\left(\frac{\mathrm{d}p_i(\xi)}{\mathrm{d}\xi} p_k(\xi) q_j(\eta)\frac{\mathrm{d}q_h(\eta)}{\mathrm{d}\eta} + \frac{\mathrm{d}p_k(\xi)}{\mathrm{d}\xi} p_i(\xi) q_h(\eta)\frac{\mathrm{d}q_j(\eta)}{\mathrm{d}\eta}\right)\Bigg\} |\mathbf{J}|\, \mathrm{d}\xi\, \mathrm{d}\eta. \qquad \text{(C.3)}
\end{aligned}$$

Finally, one obtains

$$\frac{\partial U_{\max}}{\partial c_{ij}} = \frac{1}{2}\left\{\sum_{k,h=1}^{M,N} c_{kh}\left[\sum_{m=1}^{15} P_{ijkh,m}(\xi,\eta)\right]\right\}, \qquad \text{(C.4)}$$

where

$$P_{ijkh,1}(\xi,\eta) = \int_{-1}^{1}\int_{-1}^{1} S_1 2\frac{\mathrm{d}^2 p_i(\xi)}{\mathrm{d}\xi^2}\frac{\mathrm{d}^2 p_k(\xi)}{\mathrm{d}\xi^2} q_j(\eta) q_h(\eta)\, |\mathbf{J}|\, \mathrm{d}\xi\, \mathrm{d}\eta,$$

$$P_{ijkh,2}(\xi,\eta)=\int_{-1}^{1}\int_{-1}^{1} S_2 2p_i(\xi)p_k(\xi)\frac{\mathrm{d}^2q_j(\eta)}{\mathrm{d}\eta^2}\frac{\mathrm{d}^2q_h(\eta)}{\mathrm{d}\eta^2}\mid \mathbf{J}\mid \mathrm{d}\xi\,\mathrm{d}\eta,$$

$$P_{ijkh,3}(\xi,\eta)=\int_{-1}^{1}\int_{-1}^{1} S_3\left[\frac{\mathrm{d}^2p_i(\xi)}{\mathrm{d}\xi^2}p_k(\xi)\frac{\mathrm{d}^2q_j(\eta)}{\mathrm{d}\eta^2}q_h(\eta)+\frac{\mathrm{d}^2p_k(\xi)}{\mathrm{d}\xi^2}p_i(\xi)\frac{\mathrm{d}^2q_h(\eta)}{\mathrm{d}\eta^2}q_j(\eta)\right]\mid \mathbf{J}\mid \mathrm{d}\xi\,\mathrm{d}\eta,$$

$$P_{ijkh,4}(\xi,\eta)=\int_{-1}^{1}\int_{-1}^{1} S_4 2\frac{\mathrm{d}p_i(\xi)}{\mathrm{d}\xi}\frac{\mathrm{d}p_k(\xi)}{\mathrm{d}\xi}\frac{\mathrm{d}q_j(\eta)}{\mathrm{d}\eta}\frac{\mathrm{d}q_h(\eta)}{\mathrm{d}\eta}\mid \mathbf{J}\mid \mathrm{d}\xi\,\mathrm{d}\eta,$$

$$P_{ijkh,5}(\xi,\eta)=\int_{-1}^{1}\int_{-1}^{1} S_5\left[\frac{\mathrm{d}^2p_i(\xi)}{\mathrm{d}\xi^2}\frac{\mathrm{d}p_k(\xi)}{\mathrm{d}\xi}q_j(\eta)\frac{\mathrm{d}q_h(\eta)}{\mathrm{d}\eta}+\frac{\mathrm{d}^2p_k(\xi)}{\mathrm{d}\xi^2}\frac{\mathrm{d}p_i(\xi)}{\mathrm{d}\xi}q_h(\eta)\frac{\mathrm{d}q_j(\eta)}{\mathrm{d}\eta}\right]\mid \mathbf{J}\mid \mathrm{d}\xi\,\mathrm{d}\eta,$$

$$P_{ijkh,6}(\xi,\eta)=\int_{-1}^{1}\int_{-1}^{1} S_6\left[p_i(\xi)\frac{\mathrm{d}p_k(\xi)}{\mathrm{d}\xi}\frac{\mathrm{d}^2q_j(\eta)}{\mathrm{d}\eta^2}\frac{\mathrm{d}q_h(\eta)}{\mathrm{d}\eta}+p_k(\xi)\frac{\mathrm{d}p_i(\xi)}{\mathrm{d}\xi}\frac{\mathrm{d}^2q_h(\eta)}{\mathrm{d}\eta^2}\frac{\mathrm{d}q_j(\eta)}{\mathrm{d}\eta}\right]\mid \mathbf{J}\mid \mathrm{d}\xi\,\mathrm{d}\eta,$$

$$P_{ijkh,7}(\xi,\eta)=\int_{-1}^{1}\int_{-1}^{1} S_7 q_j(\eta)q_h(\eta)\left[\frac{\mathrm{d}^2p_i(\xi)}{\mathrm{d}\xi}\frac{\mathrm{d}p_k(\xi)}{\mathrm{d}\xi}+\frac{\mathrm{d}^2p_k(\xi)}{\mathrm{d}\xi}\frac{\mathrm{d}p_i(\xi)}{\mathrm{d}\xi}\right]\mid \mathbf{J}\mid \mathrm{d}\xi\,\mathrm{d}\eta,$$

$$P_{ijkh,8}(\xi,\eta)=\int_{-1}^{1}\int_{-1}^{1} S_8 p_i(\xi)p_k(\xi)\left[\frac{\mathrm{d}^2q_j(\eta)}{\mathrm{d}\eta^2}\frac{\mathrm{d}q_h(\eta)}{\mathrm{d}\eta}+\frac{\mathrm{d}^2q_h(\eta)}{\mathrm{d}\eta^2}\frac{\mathrm{d}q_j(\eta)}{\mathrm{d}\eta}\right]\mid \mathbf{J}\mid \mathrm{d}\xi\,\mathrm{d}\eta,$$

$$P_{ijkh,9}(\xi,\eta)=\int_{-1}^{1}\int_{-1}^{1} S_9\left[\frac{\mathrm{d}^2p_i(\xi)}{\mathrm{d}\xi^2}p_k(\xi)q_j(\eta)\frac{\mathrm{d}q_h(\eta)}{\mathrm{d}\eta}+\frac{\mathrm{d}^2p_k(\xi)}{\mathrm{d}\xi^2}p_i(\xi)q_h(\eta)\frac{\mathrm{d}q_j(\eta)}{\mathrm{d}\eta}\right]\mid \mathbf{J}\mid \mathrm{d}\xi\,\mathrm{d}\eta,$$

$$P_{ijkh,10}(\xi,\eta)=\int_{-1}^{1}\int_{-1}^{1} S_{10}\left[p_i(\xi)\frac{\mathrm{d}p_k(\xi)}{\mathrm{d}\xi}\frac{\mathrm{d}^2q_j(\eta)}{\mathrm{d}\eta^2}q_h(\eta)+p_k(\xi)\frac{\mathrm{d}p_i(\xi)}{\mathrm{d}\xi}\frac{\mathrm{d}^2q_h(\eta)}{\mathrm{d}\eta^2}q_j(\eta)\right]\mid \mathbf{J}\mid \mathrm{d}\xi\,\mathrm{d}\eta,$$

$$P_{ijkh,11}(\xi,\eta)=\int_{-1}^{1}\int_{-1}^{1} S_{11}\frac{\mathrm{d}p_i(\xi)}{\mathrm{d}\xi}\frac{\mathrm{d}p_k(\xi)}{\mathrm{d}\xi}\left[\frac{\mathrm{d}q_j(\eta)}{\mathrm{d}\eta}q_h(\eta)+\frac{\mathrm{d}q_h(\eta)}{\mathrm{d}\eta}q_j(\eta)\right]\mid \mathbf{J}\mid \mathrm{d}\xi\,\mathrm{d}\eta,$$

$$P_{ijkh,12}(\xi,\eta)=\int_{-1}^{1}\int_{-1}^{1} S_{12}\frac{\mathrm{d}q_j(\eta)}{\mathrm{d}\eta}\frac{\mathrm{d}q_h(\eta)}{\mathrm{d}\eta}\left[\frac{\mathrm{d}p_i(\xi)}{\mathrm{d}\xi}p_k(\xi)+\frac{\mathrm{d}p_k(\xi)}{\mathrm{d}\xi}p_i(\xi)\right]\mid \mathbf{J}\mid \mathrm{d}\xi\,\mathrm{d}\eta,$$

$$P_{ijkh,13}(\xi,\eta)=\int_{-1}^{1}\int_{-1}^{1} S_{13}2\frac{\mathrm{d}p_i(\xi)}{\mathrm{d}\xi}\frac{\mathrm{d}p_k(\xi)}{\mathrm{d}\xi}q_j(\eta)q_h(\eta)\mid \mathbf{J}\mid \mathrm{d}\xi\,\mathrm{d}\eta,$$

$$P_{ijkh,14}(\xi,\eta)=\int_{-1}^{1}\int_{-1}^{1} S_{14}2p_i(\xi)p_k(\xi)\frac{\mathrm{d}q_j(\eta)}{\mathrm{d}\eta}\frac{\mathrm{d}q_h(\eta)}{\mathrm{d}\eta}\mid \mathbf{J}\mid \mathrm{d}\xi\,\mathrm{d}\eta,$$

$$P_{ijkh,15}(\xi,\eta)=\int_{-1}^{1}\int_{-1}^{1} S_{15}\left[\frac{\mathrm{d}p_i(\xi)}{\mathrm{d}\xi}p_k(\xi)q_j(\eta)\frac{\mathrm{d}q_h(\eta)}{\mathrm{d}\eta}+\frac{\mathrm{d}p_k(\xi)}{\mathrm{d}\xi}p_i(\xi)q_h(\eta)\frac{\mathrm{d}q_j(\eta)}{\mathrm{d}\eta}\right]\mid \mathbf{J}\mid \mathrm{d}\xi\,\mathrm{d}\eta.$$

In the same manner, replacing the approximating function (15) into the expression of the maximum kinetic energy (11) one obtains

$$T_{\max} = \frac{h\rho\omega^2}{2}\int_{-1}^{1}\int_{-1}^{1}\left(\sum_{i,j=1}^{N,M} c_{ij}p_i(\xi)q_j(\eta)\right)^2 \mid \mathbf{J} \mid \mathrm{d}\xi\,\mathrm{d}\eta$$
$$= \frac{h\rho\omega^2}{2}\int_{-1}^{1}\int_{-1}^{1}\left(\sum_{k,h=1}^{N,M}\sum_{r,s=1}^{N,M} c_{kh}c_{rs}p_k(\xi)q_h(\eta)p_r(\xi)q_s(\eta)\right) \mid \mathbf{J} \mid \mathrm{d}\xi\,\mathrm{d}\eta. \tag{C.5}$$

Then, the derivation of Eq. (C.5) with respect to each coefficient c_{ij}, $i,j = 1,\ldots,N,M$ leads to

$$\frac{\partial T_{\max}}{\partial c_{ij}} = \frac{\rho h}{2}\omega^2\left\{2\int_{-1}^{1}\int_{-1}^{1}\sum_{k,h=1}^{N,M} c_{kh}p_i(\xi)p_k(\xi)q_j(\eta)q_h(\eta) \mid \mathbf{J} \mid \mathrm{d}\xi\,\mathrm{d}\eta\right\}. \tag{C.6}$$

Finally, replacing the approximating function (15) into the expression of the potential energy (12) one obtains

$$V = -\int_{-1}^{1}\int_{-1}^{1} q(\xi,\eta)\left(\sum_{i,j=1}^{N,M} c_{ij}p_i(\xi)q_j(\eta)\right) \mid \mathbf{J} \mid \mathrm{d}\xi\,\mathrm{d}\eta. \tag{C.7}$$

The derivation of Eq. (C.7) with respect to each coefficient c_{ij}, $i,j = 1,\ldots,N,M$ leads to

$$\frac{\partial V}{\partial c_{ij}} = -\left\{\int_{-1}^{1}\int_{-1}^{1} q(\xi,\eta)p_i(\xi)q_j(\eta) \mid \mathbf{J} \mid \mathrm{d}\xi\,\mathrm{d}\eta\right\}. \tag{C.8}$$

Eqs. (C.4), (C.6) and (C.8) leads to the governing equations (20) and (21) established in the main text.

References

[1] S. Timoshenko, S. Woinowsky-Krieger, Theory of Plates and Shells, McGraw-Hill, New York, 1959.
[2] A.W. Leissa, Vibration of plates (NASA SP-160), Office of Technology Utilization, NASA, Washington, DC, 1969.
[3] A.W. Leissa, Recent studies in plate vibrations: 1981–1985. Part I: Classical theory, The Shock and Vibration Digest 19 (1987) 11–18.
[4] R.D. Blevins, Formulas for natural frequency and mode shape, Krieger Publishing Company, Malabar, FL, 1993.
[5] C.W. Bert, Research on dynamics of composite and sandwich plates, The Shock and Vibration Digest (1982) 17–34.
[6] C.W. Bert, Research on dynamics behaviour of composite and sandwich plates—V: Part I, The Shock and Vibration Digest 23 (1991) 3–14.
[7] C.W. Bert, Research on dynamics behaviour of composite and sandwich plates—V: Part II, The Shock and Vibration Digest 23 (1991) 9–21.
[8] O.C. Zienkiewicz, R.L. Taylor, The Finite Element Method, fourth ed., McGraw-Hill, New York, 1991.
[9] J.N. Reddy, Finite Element Method, second ed., McGraw-Hill, New York, 1993.
[10] T.M. Hrudey, M.M. Harbok, Singularity finite elements for plate bending, J. Engrg. Mech. ASCE 112 (1986) 666–681.
[11] W.Y. Ly, Y.K. Cheung, E.G. Tham, Spline finite strip analysis of general plates, J. Engrg. Mech. ASCE 112 (1986) 43–54.
[12] Y.K. Cheung, L.G. Tham, W.Y. Li, Free vibration and static analysis of general plate by spline finite strip, Computat. Mech. 3 (1988) 187–197.
[13] H.Y. Sheng, J.Q. Ye, A state space finite element for laminated composite plates, Comput. Methods Appl. Mech. Engrg. 191 (2002) 4259–4276.
[14] K. Rektorys, Variational Methods in Mathematics, Science and Engineering, Reidel Co., Dordrecht, 1980.
[15] R.B. Bhat, Plate deflection using orthogonal polynomials, J. Engrg. Mech. ASCE 101 (1985) 1301–1309.
[16] R.B. Bhat, Natural frequencies of rectangular plates using characteristic orthogonal polynomials in Rayleigh–Ritz method, J. Sound Vibr. 102 (1985) 493–499.
[17] K.M. Liew, K.Y. Lam, A Rayleigh–Ritz approach to transverse vibration of isotropic and anisotropic trapezoidal plates using orthogonal plate functions, Int. J. Solids Struct. 27 (1991) 189–203.
[18] K.M. Liew, Response of plates of arbitrary shape subject to static loading, J. Engrg. Mech. 118 (1992) 1783–1794.
[19] K.M. Liew, Vibration of symmetrically laminated cantilever plates, Int. J. Mech. Sci. 34 (1992) 299–308.

[20] K.M. Liew, C.W. Lim, Vibratory characteristics of general laminates. I: Symmetric trapezoids, J. Sound Vibr. 183 (1995) 615–642.
[21] K.M. Liew, K.Y. Lam, S.T. Chow, Free vibration analysis of rectangular plates using orthogonal plate function, Comput. Struct. 34 (1990) 79–85.
[22] K.M. Liew, K.Y. Lam, Application of two-dimensional orthogonal plate function to flexural vibration of skew plates, J. Sound Vibr. 139 (1990) 241–252.
[23] S.T. Chow, K.M. Liew, K.Y. Lam, Transverse vibration of symmetrically laminated rectangular composite plates, Compos. Struct. 20 (1992) 213–226.
[24] K.M. Liew, Vibration of symmetrically laminated cantilever trapezoidal composite plates, Int. J. Mech. Sci. 34 (1992) 299–308.
[25] C.W. Lim, K.M. Liew, Vibration of pretwisted cantilever trapezoidal symmetric laminates, Acta Mech. 111 (1995) 193–208.
[26] C.W. Lim, K.M. Liew, S. Kitipornchai, Vibration of arbitrarily laminated plates of general trapezoidal planform, J. Acoust. Soc. Am. 100 (1996) 3674–3685.
[27] K.M. Liew, C.W. Lim, Vibratory characteristics of pretwisted cantilever trapezoids of unsymmetric laminates, AIAA J. 34 (1996) 1041–1050.
[28] C.W. Lim, S. Kitipornchai, K.M. Liew, A free vibration analysis of doubly connected super-elliptical laminated composite plates, Compos. Sci. Technol. 58 (1998) 435–445.
[29] J.N. Reddy, Mechanics of Laminated Anisotropic Plates: Theory and Analysis, CRC Press, Boca Raton, FL, 1997.
[30] J.M. Whitney, Structural Analysis of Laminated Anisotropic Plates, Technomic Publishing Co. Inc., Pennsylvania, USA, 1987.
[31] L.G. Nallim, Mechanics of Anisotropic Plates: A Variational Approach, Doctors Thesis, National University of Salta, 2003.
[32] R.O. Grossi, L.G. Nallim, Boundary and eigenvalue problems for generally restrained anisotropic plates, J. Multi-body Dyn. 217 (2003) 241–251.
[33] L. Kantorovich, V. Krylov, Approximate Methods of Higher Analysis, Interscience Publishers, 1964.
[34] S. Mikhlin, Variational Methods of Mathematical Physics, Mac Millan Co., New York, 1964.
[35] L.G. Nallim, R.O. Grossi, On the use of orthogonal polynomials in the study of anisotropic plates, J. Sound Vibr. 264 (2003) 1201–1207.
[36] S. Wang, Vibration of thin skew fibre reinforced composite laminates, J. Sound Vibr. 201 (1997) 335–352.
[37] G. Romero, L. Alvarez, E. Alanís, L. Nallim, R. Grossi, Study of a vibrating plate: comparison between experimental (ESPI) and analytical results, Optics Lasers Engrg. 40 (2003) 81–90.